

# Ordered phases and phase transitions in the fully frustrated $XY$ model on a honeycomb lattice

S. E. Korshunov

*L. D. Landau Institute for Theoretical Physics RAS, 142432 Chernogolovka, Russia*

(Received 16 December 2011; published 26 April 2012)

The phase diagram of the fully frustrated  $XY$  model on a honeycomb lattice is shown to incorporate three different ordered phases. In the most unusual of them, a long-range order is related not to the dominance of a particular periodic vortex pattern but to the orientation of the zero-energy domain walls separating domains with different orientations of vortex stripes. The phase transition leading to the destruction of this phase can be associated with the appearance of free fractional vortices and is of the first order. The stabilization of the two other ordered phases (existing at lower temperatures) relies on a positive contribution to the domain-wall free energy induced by the presence of spin waves. This effect has a substantial numerical smallness, in accordance with which these two phases can be observed only in the systems of really macroscopic sizes. In physical systems (like magnetically frustrated Josephson junction arrays and superconducting wire networks), the presence of additional interactions must lead to a better stabilization of a phase with a long-range order in terms of vortex pattern and improve the possibilities of its observation.

DOI: [10.1103/PhysRevB.85.134526](https://doi.org/10.1103/PhysRevB.85.134526)

PACS number(s): 75.10.Hk, 64.60.De, 74.81.Fa

## I. INTRODUCTION

A uniformly frustrated  $XY$  model can be defined by the Hamiltonian

$$H = \sum_{(jj')} V(\varphi_{j'} - \varphi_j - A_{jj'}), \quad (1a)$$

where the interaction of the variables  $\varphi_j$  defined on the sites  $j$  of some regular two-dimensional lattice is described by the periodic function

$$V(\theta) = -J \cos \theta, \quad (1b)$$

$J > 0$  is the coupling constant, and the summation is performed over all pairs of nearest neighbors ( $jj'$ ) on the lattice. The nonfluctuating (quenched) variables  $A_{jj'} \equiv -A_{j'j}$  defined on lattice bonds have to satisfy the constraint

$$\sum_{\square\alpha} A_{jj'} = 2\pi f \pmod{2\pi} \quad (1c)$$

on all lattice plaquettes. The notation  $\square\alpha$  below the sign of summation implies the directed sum of variables  $A_{jj'} \equiv -A_{j'j}$  over the perimeter of plaquette  $\alpha$  in the counterclockwise direction. For  $f = 0$  the model defined by Eqs. (1) is isomorphic to the conventional  $XY$  model (without frustration), whereas for  $f = \frac{1}{2}$  (the maximal irreducible value of  $f$ , see Ref. 1) this model is called fully frustrated.

Since the 1980s, the uniformly frustrated and, especially, the fully frustrated  $XY$  models on various lattices have been studied rather intensively (for reviews, see Refs. 2 and 3), mostly in relation with experiments on Josephson junction arrays.<sup>4</sup> In these artificial superconducting systems variables  $\varphi_j$  can be associated with the phases of the superconducting order parameter on different superconducting grains forming an array, and  $A_{ij}$  is related to the vector potential of a uniform magnetic field, whose magnitude corresponds to having  $f$  superconducting flux quanta per lattice plaquette. The form of Eq. (1c) corresponds to taking into account only the external magnetic field and neglecting the field of weak currents flowing in the junctions. Planar magnets with odd number of antiferromagnetic bonds per plaquette<sup>5</sup> (for example, an

antiferromagnet with triangular lattice) are also described by the fully frustrated  $XY$  models. The recent renewal of the interest to the fully frustrated Josephson junction arrays has been related to their possible application for the creation of topologically protected quantum bits.<sup>6</sup>

In a typical situation, the energy of each of the Josephson junctions forming an array as a function of the gauge-invariant phase difference,

$$\theta_{jj'} = \varphi_{j'} - \varphi_j - A_{jj'}, \quad (2)$$

is indeed rather accurately described by the function of Eq. (1b). On the other hand, a magnetically frustrated network of thin superconducting wires can be described<sup>3</sup> in the London limit (when the amplitude of the superconducting order parameter can be assumed to be constant along the wires) by the same Hamiltonian (1a) with  $V(\theta)$  replaced by the so-called Berezinskii-Villain interaction<sup>7,8</sup> having the same symmetry and periodicity as  $V(\theta)$ ; see Appendix A. The fully frustrated  $XY$  model with the Berezinskii-Villain interaction is more convenient for a theoretical analysis, because its partition function can be rigorously transformed into that of a Coulomb gas with half-integer charges<sup>9</sup> (Appendix A gives more details). In a number of cases it can be expected that the main features of the frustrated  $XY$  models with the conventional and with the Berezinskii-Villain interaction are the same.

The ground states of the fully frustrated  $XY$  models are characterized by the coexistence of the continuous  $U(1)$  degeneracy (related to the possibility of the simultaneous rotation of all phases) with a discrete one, whose nature depends on the structure of the lattice. Accordingly, the fully frustrated  $XY$  models allow in addition to the phase transition related to unbinding of vortex pairs also for the existence of other phase transitions related to the disordering of the discrete degrees of freedom. The main question in such a situation is what is the sequence and the nature of these phase transitions.

The most thoroughly studied examples of the fully frustrated  $XY$  models are the models on square and triangular lattices. In both of them the ground states are characterized

by a regular alternation of the plaquettes with positive and negative vorticities. Accordingly, the discrete degeneracy of the ground states is twofold, that is, the simplest one that is possible. However, it took about two decades before it was firmly understood<sup>3,10</sup> why the Berezinskii-Kosterlitz-Thouless transition related to the unbinding of vortex pairs has to take place in these models at lower temperatures than the second phase transition related to the proliferation of the Ising-type domain walls. Due to a strong mutual influence of the two transitions (which are situated rather close to each other), a convincing numerical demonstration of the Ising nature of one of them has required very substantial efforts.<sup>2,11</sup>

The properties of the fully frustrated  $XY$  model on a honeycomb lattice are not so well understood. The family of its ground state is known to have an infinite discrete degeneracy,<sup>12</sup> which can be conveniently described in terms of the formation of zero-energy domain walls parallel to each other.<sup>13,14</sup> The analysis of the half-integer Coulomb gas on a triangular lattice (a representation of the considered  $XY$  model in terms of vortices) has revealed<sup>15</sup> that in this system the formation of a domain with a different charge pattern can cost only a finite energy even when the size of this domain is arbitrary large. This has led the authors of Ref. 15 to the conclusion on the absence of a long-range order at any nonzero temperature  $T$ .

This conclusion is not directly applicable to the fully frustrated  $XY$  model with the interaction given by Eq. (1b) because at  $T > 0$  the zero-energy domain walls acquire a positive free energy  $f_{\text{DW}}$  originating from the difference in the free energy of the continuous fluctuations (spin waves).<sup>14</sup> However, the effect is very weak and according to the estimates in Ref. 14 can manifest itself only if the size of the system  $L$  substantially exceeds  $L_c \gtrsim 10^5$ , which makes it unobservable in real and numerical experiments on systems with  $L \lesssim L_c$ .

Nonetheless, up to now it has remained unclarified if, in situations when  $f_{\text{DW}}$  is absent (as it happens in the case of the Berezinskii-Villain interaction) or can be neglected, the system can still demonstrate a phase transition related to the continuous degrees of freedom or the destruction of the long-range order in terms of vortex pattern prevents the possibility of such a transition. The available numerical data<sup>12,15-18</sup> does not lead to a unique conclusion and allows for different interpretations, including the existence of a spin-glass transition.<sup>17</sup>

In this work we reexamine the fully frustrated  $XY$  model on a honeycomb lattice with the aim of finding an answer to this question, as well as establishing what is the nature of the phase transition (transitions) induced by the positiveness of  $f_{\text{DW}}$ . Our main conclusions can be formulated as follows.

Even when  $f_{\text{DW}}$  is equal to zero (or can be neglected), this does not mean the complete absence of the long-range order at any nonzero temperature. In a such a situation, the long-range order existing at low temperatures is related not to the dominance of a particular vortex pattern but to a preferable orientation of the zero-energy domain walls.

The phase transition leading to the destruction of this long-range order is related to the appearance of a finite concentration of unpaired fractional vortices with topological charges  $q = \pm \frac{1}{8}$ . The fractional vortices are located at the nodes of the domain-wall network existing in the system with  $f_{\text{DW}} = 0$  at any temperature; however, at low temperatures they have to

be bound in pairs, which imposes the existence of a preferable orientations of domain walls.

In the model with the conventional interaction  $V(\theta) = -J \cos \theta$  which at  $T > 0$  has small but positive  $f_{\text{DW}}$  (induced by spin waves), the increase of temperature leads to the sequence of three phase transitions. However, the two of them require for their observation very large systems with  $L \gg L_c \sim 10^7$ . In physical systems like magnetically frustrated Josephson junction arrays and superconducting wire networks, the value of  $L_c$  will be lower due to the presence of other mechanisms for the removal of the accidental degeneracy.

Although the lowest-temperature phase transition (whose critical temperature tends to zero when  $f_{\text{DW}} \rightarrow 0$ ) consists in the appearance of domain walls, it does not lead to the destruction of the long-range order in terms of vortex pattern. On the contrary, it is related to a partial restoration of the continuous  $U(1)$  symmetry. This phase transition belongs to the Ising universality class, whereas the two other transitions mentioned above must be of the first order.

A more detailed summary of the phase diagram of the fully frustrated  $XY$  model on a honeycomb lattice and of the properties of different phases and phase transitions is presented in the concluding Sec. VIII. It also compares our results with that of other works and discusses their relevance for some experimental situations and other uniformly frustrated  $XY$  models that allow for the formation of parallel zero-energy domain walls.

## II. ZERO-TEMPERATURE ANALYSIS

### A. The ground states

When speaking about both global and local minima of the Hamiltonian of an  $XY$  model it is convenient to characterize them in terms of vorticities of different plaquettes. Vorticity  $v_\alpha$  of plaquette  $\alpha$  can be defined as the directed sum over the perimeter of this plaquette of the gauge-invariant phase differences  $\theta_{jj'} = \varphi_{j'} - \varphi_j - A_{jj'}$  reduced to the interval  $(-\pi, \pi)$ . Here and below we use Greek indices for labeling the plaquettes, each of which can be associated with a particular site of the triangular lattice  $\mathcal{T}$  dual to the original honeycomb lattice  $\mathcal{H}$ .

In the fully frustrated  $XY$  model on a honeycomb lattice, variables  $v_\alpha$  can acquire the values  $\pm\pi, \pm 3\pi, \pm 5\pi$ . Since the main role in the thermodynamics is played by the minima of the Hamiltonian of Eq. (1) with  $v_\alpha = \pm\pi$  (as well as by fluctuations in the vicinities of these minima), one often speaks not about vorticities but about chiralities  $\sigma_\alpha = v_\alpha/\pi = \pm 1$  of different plaquettes. The knowledge of the chiralities of all plaquettes is sufficient for restoring (up to a global rotation) the values of phase variables  $\varphi_j$  in the minimum of the Hamiltonian that can be associated with this particular configuration of chiralities.

In all ground states of the fully frustrated  $XY$  model on a honeycomb lattice the plaquettes with different signs of chirality are separated by the bonds with  $\theta_{jj'} = \pm\pi/4$ , whereas the plaquettes with the same sign of chirality are separated by the bonds with  $\theta_{jj'} = 0$ . In Fig. 1 showing some of the ground states the plaquettes with positive (negative) chirality

are shaded (unshaded), whereas the bonds with  $\theta_{jj'} = \pm\pi/4$  are shown by arrows. On any bond with an arrow,  $\theta_{jj'}$  is equal to  $+\pi/4$  if the arrow is directed from site  $j$  to site  $j'$  and to  $-\pi/4$  in the opposite case.

Figure 1(a) shows an example of the ground state with the simplest possible structure. In this state the plaquettes with the same sign of vorticity form parallel straight stripes. Accordingly, such states are called below the striped states. The set of striped states is characterized by a sixfold discrete degeneracy related to the possibilities of shifting and rotating vortex pattern. Naturally, it also has the continuous  $U(1)$  degeneracy related to the simultaneous rotation of all phases, but in the following the term *striped state* will always refer just to the configuration of chiralities, without specifying the phases.

Striped states allow for the formation of domain walls (separating different realizations of such states) that cost no energy.<sup>13</sup> An example of such a zero-energy domain wall (ZEDW) is shown in Fig. 1(b). An arbitrary number of ZEDWs separated by arbitrary distances can be introduced into the system in parallel to each other, as shown in Fig. 1(c).

The only possible intersection of ZEDWs that does not cost extra energy is shown in Fig. 1(d). Since each ZEDW can be ascribed a particular direction in accordance with the orientation of the angle made by the stripes, as shown in Fig. 1, it is clear that in a ground state the system cannot contain more than one intersection of such a kind and, in the case of the periodic boundary conditions, even one is impossible. Therefore, a typical ground state contains an irregular sequence of straight ZEDWs that are parallel to each other, as shown in Fig. 1(c). The presence of a boundary between two ground states with a finite concentration of ZEDWs and different orientations of these walls would cost an amount of energy proportional to the length of this boundary.

The structure of the ground states is not sensitive to a particular form of the interaction in the Hamiltonian of the model, as soon as it is even in  $\theta$  and behaves more or less in the same way as  $V(\theta) = -J \cos \theta$  [that is, it has the single maximum at  $\theta = \pi$  and the single minimum at  $\theta = 0$  whose width is comparable with the period of  $V(\theta)$ ]. For example, it can be also the Berezinskii-Villain interaction defined by Eq. (A2) or the piecewise parabolic interaction (the zero-temperature limit of the Berezinskii-Villain interaction).

## B. Zero-energy domain walls and long-range order

If domain walls separating different striped states would have a positive energy per unit length, at zero temperature the system would be frozen in one of the six striped states. In terms of chiralities  $\sigma_\alpha$ , the order parameter corresponding to the corresponding long-range order (LRO) can be written as

$$S = \sum_{n=1}^3 e^{i \frac{2\pi n}{3}} \sum_{\alpha} s_{n,\alpha}, \quad s_{n,\alpha} = \sigma_\alpha \exp \frac{i \mathbf{Q}_n \mathbf{r}_\alpha}{2}. \quad (3)$$

Here and below  $\mathbf{r}_\alpha$  denotes the positions of the sites  $\alpha$  of the dual triangular lattice  $\mathcal{T}$  that can be associated with the plaquettes of the original honeycomb lattice  $\mathcal{H}$ , whereas  $\mathbf{Q}_n$  (with  $n = 1, 2, 3$  and  $\mathbf{Q}_1 + \mathbf{Q}_2 + \mathbf{Q}_3 = 0$ ) are the three reciprocal vectors of  $\mathcal{T}$ . In any of the striped states one of the three sums  $S_n \equiv \sum_{\alpha} s_{n,\alpha}$  grows with size of the system as  $S_n = \pm N$  ( $N$  being the total number of the plaquettes in the system), whereas the two other are equal to zero. The correlation function

$$C_{\text{ch}}(\mathbf{r}_\alpha - \mathbf{r}_\beta) = \langle \sigma_\alpha \sigma_\beta \rangle, \quad (4)$$

where the average is taken over the six striped vortex patterns, has an oscillating behavior, namely if a triangular lattice  $\mathcal{T}$  is partitioned into four equivalent triangular sublattices, then  $C_{\text{ch}}(\mathbf{r}_\alpha - \mathbf{r}_\beta)$  is equal to 1 when  $\alpha$  and  $\beta$  belong to the same sublattice and to  $-1/3$  when they belong to different sublattices.

When the domain walls shown in Fig. 1 cost no energy, the oscillating behavior (without a decay at  $|\mathbf{r}_\alpha - \mathbf{r}_\beta| \rightarrow \infty$ ) of the correlation function of Eq. (4) (where the average now has to be taken over the infinite set of the ground states) is retained only when  $\alpha$  and  $\beta$  belong to the same column of sites on  $\mathcal{T}$ , that is, when vector  $\mathbf{r}_\alpha - \mathbf{r}_\beta$  is directed along  $\mathbf{e}_n$ , one of the three lattice vectors of  $\mathcal{T}$  ( $\mathbf{e}_1 + \mathbf{e}_2 + \mathbf{e}_3 \equiv 0$ ). In such a case, in one-third of the ground states, the line connecting  $\alpha$  and  $\beta$  cannot be crossed by any domain walls and, therefore, the product  $\sigma_\alpha \sigma_\beta$  depends only on the distance between  $\alpha$  and  $\beta$ . For all other directions of  $\mathbf{r}_\alpha - \mathbf{r}_\beta$ , the correlations of  $\sigma_\alpha$  and  $\sigma_\beta$  are absent, which leads to

$$\langle |S|^2 \rangle \propto N. \quad (5)$$

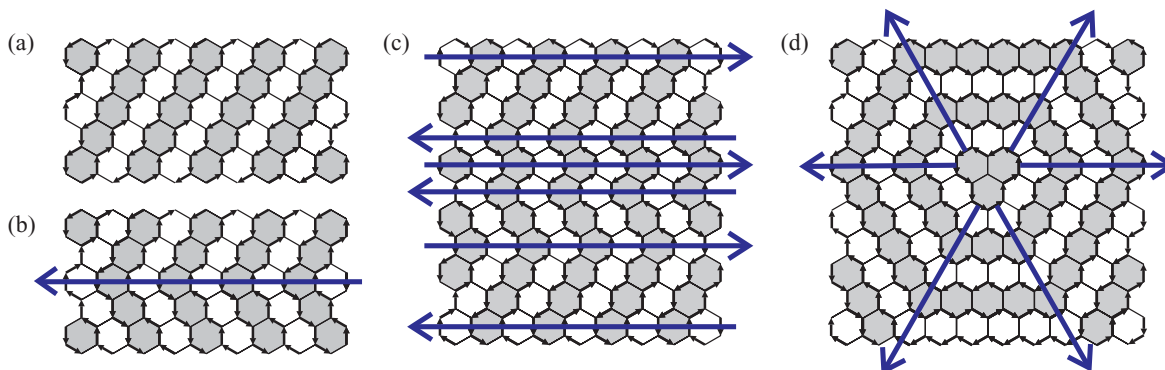


FIG. 1. (Color online) The ground states of the FFXY model on a honeycomb lattice: (a) a striped state; (b) a state with a single zero-energy domain wall separating two different striped states; (c) a typical ground state with an irregular sequence of parallel domain walls; (d) the only possible intersection of domain walls that does not cost extra energy. The plaquettes with positive (negative) chirality are shaded (unshaded).

This means that the long-range order in terms of  $s_{n,\alpha}$  is destroyed. It is worthwhile to emphasize explicitly that the dependence in Eq. (5) is not a consequence of algebraic correlations of  $\sigma_\alpha$ , as it could seem from its form, but has a different origin explained above.

However, it is not difficult to note that the destruction of the long-range order is not complete. In the presence of a random sequence of straight parallel ZEDWs, the system contains the domains of only four different striped states of six, whereas the two other vortex patterns (with stripes parallel to the direction of the domain walls) are not represented at all. Therefore, in a typical ground state the system still possesses a long-range order. The most evident interpretation of this order consists in associating it with the direction of ZEDWs.

Instead of really monitoring the direction of domain walls (whose identification requires analyzing chirality patterns in rhombic clusters formed by four neighboring plaquettes), an order parameter sensitive to the direction of domain walls can be introduced by studying the distribution of energy between the bonds with different orientations. In a typical ground state the average energy of the bonds whose direction is perpendicular to the orientation of domain walls is equal to  $V(\pi/4)$ , whereas for the bonds with two other orientations it is equal to  $\frac{1}{2}[V(0) + V(\pi/4)] < V(\pi/4)$ . This allows one to introduce an order parameter as

$$D = \sum_{(jj')} \exp \left[ i \frac{2\pi n_{jj'}}{3} \right] V(\theta_{jj'}), \quad (6)$$

where the value of  $n_{jj'} = 1, 2, 3$  depends on the orientation of the bond  $(jj')$ .

Thus, the vanishing of the energy of domain walls does not lead to the complete destruction of the long-range order in the system and one can expect that there should occur a phase transition related to the destruction of the long-range order described by order parameter  $D$ . Note that  $D$  is proportional to the area of the system also when one of the six striped vortex patterns is a dominant one. However, in contrast to  $S$ , order parameter  $D$  does not allow one to distinguish between two vortex patterns that differ from each other by changing the signs of all chiralities.

### C. Phase correlations

When speaking about phase correlations, one should not forget that a change of gauge leads to the multiplication of  $\exp[i(\varphi_\alpha - \varphi_\beta)]$  by some phase factor. In accordance with that, a gauge-invariant description of phase correlations can be achieved by paying attention only to the absolute values of the standard correlation functions. For taking into account the peculiarities of the considered model, it is convenient to introduce the set of gauge-invariant phase correlation functions defined as

$$C_p(\mathbf{r}_j - \mathbf{r}_k) = |\langle \exp[ip(\varphi_j - \varphi_k)] \rangle| \quad (7)$$

and numbered by positive integer  $p$ . Another approach to introducing gauge-invariant phase correlation functions involves considering two identical but completely independent replicas of the system.<sup>19</sup>

If domain walls separating different striped states would have a positive energy per unit length, at zero temperature

there would exist a true long-range order in terms of phase variables. In particular, if the honeycomb lattice is partitioned into 32 equivalent triangular sublattices, for any two sites  $j$  and  $k$  belonging to the same sublattice,  $C_p(\mathbf{r}_j - \mathbf{r}_k)$  would be equal to 1 for any integer  $p$ . On the other hand, when  $p$  is a multiple of eight ( $p = 8p'$  with integer  $p'$ ),  $C_p(\mathbf{r}_j - \mathbf{r}_k)$  would be equal to 1 for any pair of sites. This is evident already from the fact that for  $\theta_{jj'} = 0, \pm \pi/4$  the factors  $\exp i(8\theta_{jj'})$  are always equal to 1.

For evident reasons, the presence of a random sequence of straight domain walls separating different striped states cannot change the behavior of  $C_p(\mathbf{r})$  with  $p = 8p'$ , which remain identically equal to 1. However, it leads to an exponential decay of  $C_p(\mathbf{r})$  for  $p \neq 8p'$  for all directions except those parallel to  $\mathbf{e}_n$ . For these special directions, all phase correlation functions with  $p < 8$  have an oscillating behavior. Like with chiralities, when one calculates the averages of the squares of certain Fourier transforms of  $\exp(ip\varphi_j)$  over all ground states, they diverge in a typical ground state proportionally to the area of the system, but this should not be taken for the signature of the algebraic correlations of  $\exp(ip\varphi_j)$ .

### III. REMOVAL OF THE ACCIDENTAL DEGENERACY BY SPIN WAVES

The infinite degeneracy of the ground states that manifests itself through the possibility of the formation of ZEDWs is of an accidental nature (i.e., it is not imposed by the symmetries of the system). Accordingly, it can be removed by the addition of some small interactions that preserve the symmetries of the Hamiltonian. It is also removed at a finite temperature when one takes into account the free energy of the continuous fluctuations (spin waves). This mechanism for the removal of an accidental degeneracy<sup>20,21</sup> is often referred to as ‘‘order from disorder.’’ In systems with a continuous degeneracy it is usually sufficient to compare the contributions from the harmonic fluctuations.<sup>21–23</sup>

In contrast, in the fully frustrated  $XY$  model on a honeycomb lattice the free energy of the harmonic fluctuations is exactly the same for all ground states of the model.<sup>14</sup> This is a consequence of a hidden symmetry existing in the Hamiltonian describing such fluctuations.<sup>24</sup> The difference in the spin-wave free energy appears only when one goes beyond the harmonic approximation. The analysis of the third- and fourth-order anharmonic terms reveals that the spin-wave free energy is minimal for the striped states, whereas the presence of ZEDWs adds to the free energy of the system, a positive term roughly proportional to the total length of the walls.<sup>14</sup> This allows one to ascribe to domain walls the free energy per unit length,

$$f_{\text{DW}} = \gamma T^2/J, \quad \gamma \approx 0.7 \times 10^{-4}, \quad (8)$$

where by *unit length* we mean the lattice constant of the dual triangular lattice  $a_\Delta$ . In terms of  $a_\Delta$ , the lengths of all walls are integer.

The positiveness of  $f_{\text{DW}}$  suggests that in the thermodynamic limit the free energy of a domain wall crossing the whole system is infinite and, therefore, at the lowest temperatures (at which the positiveness of  $f_{\text{DW}}$  is not killed by other types of fluctuations), such walls must be absent. This ensures the existence of the long-range order corresponding to the



dominance of one of the six equivalent striped vortex patterns. On the other hand, at any nonzero temperature the presence of spin waves leads to an algebraic decay of the correlation functions describing phase correlations.

In terms of chiralities  $\sigma_\alpha = \pm 1$  (defined on sites  $\alpha$  of the dual triangular lattice), the structure of the striped state is exactly the same as that of the ground state of the antiferromagnetic Ising model on a triangular lattice with an additional weak antiferromagnetic interaction of second neighbors.<sup>25</sup> In this model there exist two different scenarios for the disordering of the ordered state,<sup>26</sup> the choice between which depends on the relations between the coupling constants. The basic scenario consists in having a single first-order transition leading to the formation of an isotropic domain-wall network mixing the domains of all six striped states. This leads to the complete loss of the long-range order. It is interesting that this phase transition takes place when the free energy of a domain wall (per unit length) is still positive and not when it vanishes.

However, for some relations between the coupling constants the first-order transition related to the formation of a domain-wall network can be preceded by a continuous phase transition related to vanishing of the free energy of double domain walls. This phase transition leads only to a partial loss of the long-range order. Above it the threefold degeneracy with respect to the directions of stripes still persists, but the system consists of alternating domains of the two striped states with the same orientation of the stripes.<sup>26</sup>

The existence of different options suggests that in the fully frustrated  $XY$  model on a honeycomb lattice, the conclusion on how the disordering of the striped state takes place also should be based on the comparison of different mechanisms for disordering. In particular, it still remains to be established what the nature of the first (with the increase in temperature) phase transition induced by the extreme smallness of the domain-wall free energy is and whether it leads to the complete loss of the long-range order or only to its partial loss, which leaves a place for another phase transition (or transitions).

In order to answer these questions we have to understand what is the most efficient mechanism for the proliferation of domain walls. And since the decrease of the free energy of domain walls is induced by the presence on them of pointlike defects we have to find the pointlike defects that play the dominant role in the development of the domain-wall fluctuations.

#### IV. POINTLIKE DEFECTS

##### A. Conventional vortices and vortex pairs

As with any other  $XY$  model, the fully frustrated  $XY$  model on a honeycomb lattice allows for the formation of conventional vortices with integer topological charges. In particular, a vortex with topological charge  $q = \pm 1$  is created when the sign of chirality of some plaquette is flipped in comparison with what it would be in a ground state. On any contour surrounding the core of a vortex with topological charge  $q$  the deviations of the gauge-invariant phase differences  $\theta_{jj'} = \varphi_{j'} - \varphi_j - A_{jj'}$  from the values they would have in a ground state (0 or  $\pm\pi/4$ ) sum to  $2\pi q$ .

At low temperatures vortices with integer topological charges can be present in the system only in the form of small neutral pairs whose concentration at  $T \ll J$  has to be exponentially low. Below we demonstrate that all phase transitions in the considered model take place at  $T \ll J$ , when the bound pairs of integer vortices are exponentially rare and, accordingly, have no influence on the properties of the system. For this reason the presence of such pairs can be neglected.

In addition to conventional vortices, in frustrated  $XY$  models there also can exist fractional vortices localized on corners and intersections of domain walls.<sup>13,27</sup> In the situation when the energy of domain walls connecting different fractional vortices is exactly equal to zero, the energies of neutral pairs of fractional vortices will be much lower than that of pairs of conventional vortices. Accordingly, one can then expect the neutral pairs of fractional vortices to be the most important finite-energy excitations at the lowest temperatures.

##### B. Fractional vortices

In any ground state of the fully frustrated  $XY$  model on a honeycomb lattice, each plaquette has exactly two nearest neighbors with the same sign of chirality and four with the opposite sign. In such a situation the simplest idea of having a pointlike excitation consists in constructing a configuration in which one (and only one) of the plaquettes has a wrong number of neighbors with the same sign of chirality. Indeed, such configurations can be constructed, see Fig. 2, where, as in other figures below, the plaquettes with positive (negative) chiralities are marked by the presence (absence) of shading.

In particular, in Fig. 2(a) the plaquette denoted by the plus sign has three neighbors with the same sign of chirality (instead of two), whereas the analogous plaquette in Fig. 2(b) has one neighbor. In both configurations, in order to have the correct number of neighbors with the same sign of chirality on all other plaquettes, three ZEDWs have to merge at the defect.

An important property of these defects is that they are fractional vortices with topological charges  $q = \pm 1/8$ . In any ground state, the correct value of vorticity on each plaquette is achieved because, on all four bonds separating it from the plaquettes with the opposite sign of vorticity, variables  $\theta_{jj'}$  are equal either to  $+\pi/4$  or to  $-\pi/4$  and sum to  $\pm\pi$ . When the number of neighbors with the same sign of vorticity is equal to 1 or 3 (instead of 2), there appears a misfit of  $\pm\pi/4$  that has to be distributed over all six bonds surrounding the corresponding plaquette. The same misfit is also present on any closed contour surrounding the defect independently of the size of this contour, from where it is clear that the deviations of variables  $\theta_{jj'}$  from the values they would have in a ground state (0 or  $\pm\pi/4$ ) decay with the distance from the defect  $R$  as  $1/R$ . This leads to a logarithmic divergence of the energy of a single defect and a logarithmic (at large distances) interaction between such defects. In accordance with their topological charges  $q = \pm 1/8$ , the logarithmic interaction of the fractional vortices in the considered problem is 64 times smaller than that of conventional vortices with topological charges  $q = \pm 1$ .

The defect shown in Fig. 2(c) (in which the central plaquette has no neighbors with the same sign of vorticity) can be considered as an overlap of two defects of the type shown

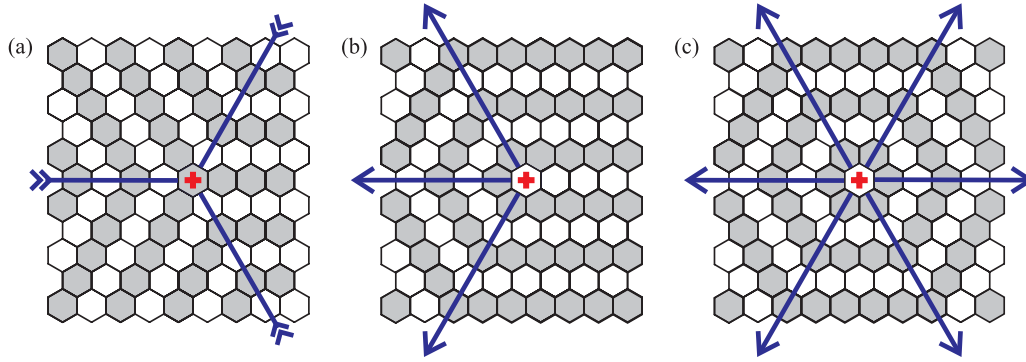


FIG. 2. (Color online) The simplest pointlike defects in which one of the plaquettes has a wrong number of neighbors with the same sign of chirality.

in Fig. 2(b). This statement applies both to the number of ZEDWs that meet at the defect and to its vorticity.

In Fig. 2 the positions of fractional vortices are denoted by the plus sign, because in all configurations shown in this figure the topological charge of the fractional vortex is positive. Below the positions of fractional vortices are denoted by pluses and minuses in accordance with the signs of their topological charges. In the case of the Berezinskii-Villain interaction, it is possible to exactly express the energy of any configuration of chiralities in terms of the pairwise interaction between fractional vortices (see Appendix B).

### C. Neutral pairs of fractional vortices

We now know how the fractional vortices look like and the next step is to find how two fractional vortices can be combined to form a neutral pair with a finite energy. Since each ZEDW can be ascribed a particular direction as shown in Figs. 1 and 2, each fractional vortex can be considered either as a “sink” [the configuration in Fig. 2(a)] or as a “source” [the configurations in Figs. 2(b) and 2(c)] of domain walls.

Apparently, in the case of periodic boundary conditions, the number of sources must be equal to the number of sinks [naturally, for the correct balance the configurations of the type shown in Fig. 2(c) have to be counted as double sources]. It is impossible to construct an isolated pair of fractional vortices from two sink configurations because the domain walls meeting in them would have to intersect each other, which would imply the existence of other defects close by. For

the same reason it is impossible to construct an isolated pair from two double sources. On the other hand, although locally a neutral pair consisting of two sources looks like a legitimate object (see Fig. 3), such pairs cannot appear because in the absence of unpaired fractional vortices there will be no sinks to compensate for these sources [in that respect they resemble the configuration shown in Fig. 1(d)].

Therefore, in a domain-wall network formed by small pairs of fractional vortices, each pair should consist of a source and a sink. Such pairs can be divided into three classes, exemplified in Fig. 4. The first of them is an intersection of a single ZEDW and a double domain wall, that is, a pair of parallel ZEDWs (which change their orientation after crossing a single wall). An example of such a pair of fractional vortices is shown in Fig. 4(a).

The second type of the fractional-vortex pairs are the bends on a double domain wall; see Fig. 4(b). For such a pair to be neutral, the distance between the two single walls forming the double wall has to be even (in the considered model it is natural to measure the distance between domain walls in units of  $h_{\Delta}$ , the height of the triangular cell of the dual lattice). If the distance between two parallel ZEDWs would be odd (for example, the minimal distance), in the configuration analogous to the one shown in Fig. 4(b) both fractional vortices would be of the same sign.

The third class of the fractional-vortex pairs corresponds to a double domain wall ending on a single domain wall; see Fig. 4(c). In this case, the distance between the two parallel ZEDWs also has to be even in order to avoid a situation when both fractional vortices in a pair are of the same sign.

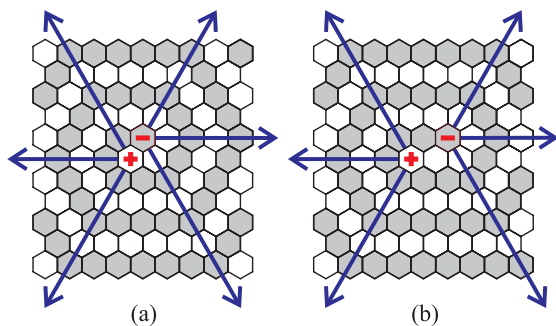


FIG. 3. (Color online) Neutral pairs of fractional vortices that cannot be present in the system in the absence of free fractional vortices.

## V. THE LOWEST-TEMPERATURE PHASE TRANSITION

When a linear defect (for example, a domain wall) has proper energy or free energy per unit length  $\epsilon$  and additionally allows for the creation of pointlike defects with energy  $E_D$ , its total free energy per unit length is given by

$$F = \epsilon - cT \ln(1 + e^{-E_D/T}) \approx \epsilon - cT e^{-E_D/T}, \quad (9)$$

where  $c$  is the number of places per unit length available for the formation of a pointlike defect and we have assumed that  $T \ll E_D$ . A natural choice for the unit length when speaking about domain walls in a lattice model is the lattice constant either of the direct or of the dual lattice, depending on whether

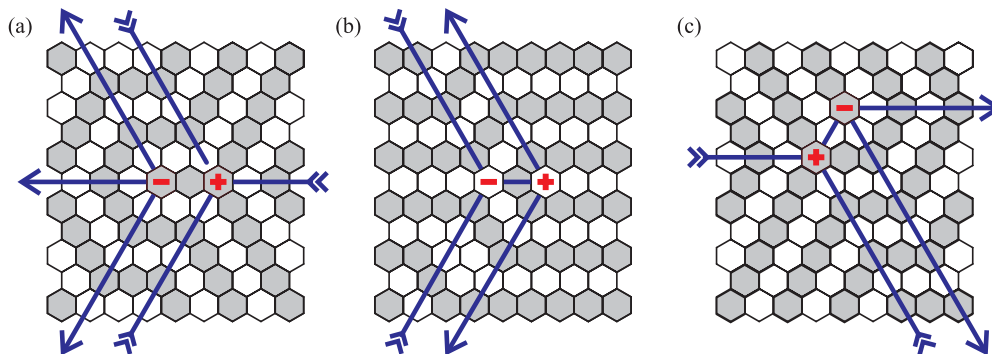


FIG. 4. (Color online) Neutral pairs of fractional vortices that can exist in the absence of free fractional vortices.

the domain walls can be associated with the bonds of the former or of the latter. Then  $c$  has to be equal either to 1 or to some simple fraction (or integer) of the order of 1. In our system, it is convenient to measure the length of domain walls in lattice constants of the dual (triangular) lattice,  $a_\Delta$ .

It follows from Eq. (9) that for  $\epsilon \ll E_D$  the temperature  $T_*$  at which  $F$  changes sign lies between  $\epsilon/c$  and  $E_D$  ( $\epsilon/c \ll T_* \ll E_D$ ) but depends on  $E_D$  much stronger than on  $\epsilon$ ,

$$T_* = \frac{E_D}{\ln(cT_*/\epsilon)}. \quad (10)$$

It is clear from Eq. (10) that the first linear defects whose free energy vanishes with the increase in temperature are those that allow for the formation of pointlike defects with the lowest energy.

It follows from the analysis of Sec. IV C that the lowest-energy pointlike excitation on a linear defect in the considered problem is a bend on a doubly spaced double domain wall (DDDW), consisting of two single domain walls separated by distance  $2h_\Delta$ ; see Fig. 4(b). A numerical minimization of energy in a finite system (complemented with the extrapolation to the infinite size) shows that in the model with  $V(\theta) = -J \cos \theta$  the energy of this defect  $E_B$  is one order of magnitude smaller than the coupling constant,  $E_B/J \approx 0.111$ . Taking for DDDW  $\epsilon = 2f_{DW}$ , with  $f_{DW}$  given by Eq. (8),  $c = 1$ , and  $E_D = E_B$ , one obtains from Eq. (10) that  $T_{c1}$ , the temperature where the free energy of a DDDW vanishes, is about 14 times lower than  $E_B$  and two orders of magnitude lower than the coupling constant,

$$T_{c1} \approx 0.81 \times 10^{-2} J. \quad (11)$$

In the vicinity of  $T_{c1}$ , the influence of the pointlike defects on the free energy of other types of domain walls can be neglected. This follows from the analysis of their energies. In particular, a bend on a double domain wall with the minimal separation between the walls,  $h_\Delta$  (a singly spaced double domain wall), contains two fractional vortices with the same sign of topological charge  $q = \pm \frac{1}{8}$ . Therefore, its energy is logarithmically divergent and the lowest-energy excitation on such a wall is not a bend but a kink formed by two bends; see Fig. 5(a). Since this object can be considered as a neutral pair of fractional vortices with topological charges  $q = \pm \frac{1}{4}$ , its energy  $E_K$  has to be larger than that of a bend on a DDDW (a neutral pair of fractional vortices with topological charges  $q = \pm \frac{1}{8}$ ). This is confirmed by a numerical calculation revealing that  $E_K \approx 0.287 J$ , that is, the energy of such a kink is 2.6 times larger than that of a bend on a DDDW. This ensures that at  $T \approx T_{c1}$  the correction to the free energy of a singly spaced double domain wall is nine orders of magnitude smaller than its bare value and, therefore, can be neglected.

A single domain wall has no possibility to make a bend, because the direction of such a wall is uniquely determined by the directions of vortex stripes in the states it separates. The simplest pointlike excitation on a single domain wall is a kink with height  $2h_\Delta$ . Such a kink is formed by four fractional vortices with  $q = \pm 1/8$  having the same sign [see Fig. 5(b)] and, therefore, has topological charge  $q = \pm \frac{1}{2}$ . Accordingly, the minimal-energy excitation on a single domain wall is a neutral pair of such kinks forming a kink of height  $4h_\Delta$ ; see Fig. 5(c). It is clear that the energy of this complex object  $E_K^s$  has to be about one order of magnitude larger than that of a bend on a DDDW (for the case of the Berezinskii-Villain

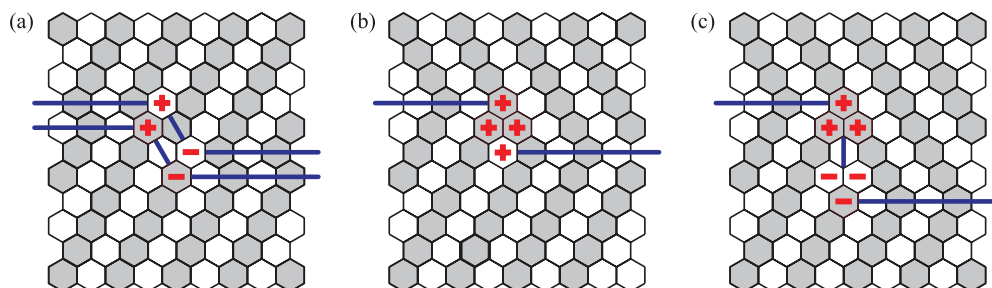


FIG. 5. (Color online) Kinks on a singly spaced double domain wall (a) and a single domain wall [(b) and (c)].

interaction, the values of  $E_B$ ,  $E_K$ ,  $E_K^s$ , and other finite-energy defects mentioned in the text can be found in Appendix B).

From this, one can conclude that in the vicinity of  $T_{c1}$  all other topological excitations save DDDWs can be neglected. Note that since the vortex patterns on the two sides of a DDDW are the same, a DDDW is not a topologically stable object and, in principle, can end somewhere; see Fig. 6(a). This is especially evident when one notices that any DDDW is nothing else but a line of plaquettes with alternating chiralities on which the signs of all chiralities are reversed. However, the states on the two sides of a DDDW are not exactly the same, namely they differ by a phase rotation by  $\pi$ . In order to compensate for this misfit an end point of a DDDW has to be a fractional vortex with topological charge  $q = \pm\frac{1}{2}$ . The same conclusion also follows from observing that an end point is formed by four fractional vortices with  $q = \pm\frac{1}{8}$  having the same sign; see Fig. 6(a).

At temperatures we are discussing, vortices with topological charges  $q = \pm\frac{1}{2}$  have to be bound in small neutral pairs. Therefore, in the nearest vicinity of any end point there always has to be present another end point with the opposite topological charge, so the two DDDWs can be considered a continuation of one another [an analogous situation is known to exist in the unfrustrated  $XY$  model in which the interaction function  $V(\theta)$  in addition to the main minimum at  $\theta = 0$  has an additional minimum at  $\theta = \pi$  with almost the same depth].<sup>28</sup> The orientation of a fluctuating DDDW is determined by the orientation of stripes in the vortex pattern on its sides, on the average such a wall will be perpendicular to the direction of stripes.

At  $T > T_{c1}$  the free energy of a single DDDW becomes negative, which suggests that there should appear a finite concentration of such walls  $\rho$  restricted by their repulsion. Since this repulsion is of contact nature, the dependence of  $\rho$  on the distance from the critical temperature can be expected to be of the Pokrovsky-Talapov<sup>29</sup> type,  $\rho \propto (T - T_{c1})^{1/2}$ .

However, in addition to the formation of infinite DDDWs the system allows also for the creation and annihilation of pairs of fluctuating DDDWs; see Fig. 6(b). This means that, in addition to infinite DDDWs crossing the whole system, there should be present finite-size defects formed by two fluctuating DDDWs, which on both sides of the defect merge together as shown in Fig. 6(b). In the theory of the commensurate-incommensurate transitions the objects where  $n$  solitons merge together are known as dislocations and the case of  $n = 2$

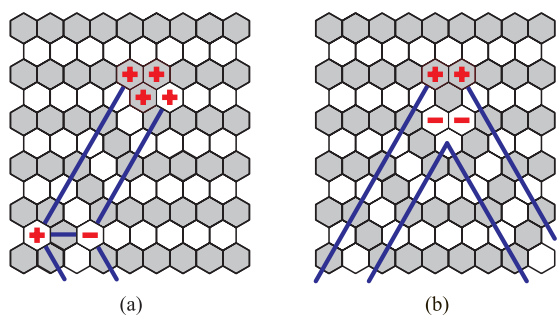


FIG. 6. (Color online) (a) An end point of a DDDW is a  $q = \pm\frac{1}{2}$  vortex; (b) an end point of a finite-size defect formed by two fluctuating DDDW.

corresponds to the double degeneracy of the ground state.<sup>30</sup> In our system, the presence of a twofold degeneracy manifests itself through the fact that the states on the two sides of a DDDW differ from each other by phase rotation by  $\pi$ . As a consequence of this, after crossing two DDDWs one returns to the same state as before. Accordingly, the phase transition related to the proliferation of DDDWs has to be of the Ising type.

Since the states on the two sides of a DDDW correspond to the same vortex pattern but differ by a phase rotation by  $\pi$ , the phase transition related to their proliferation does not destroy the long-range order in terms of chirality but leads to a partial suppression of phase correlations. In particular, an algebraic decay of correlation function  $C_1(\mathbf{r})$  is replaced by an exponential one, whereas the correlations of the double phase [described by  $C_2(\mathbf{r})$ ] remain algebraic. In the Pokrovsky-Talapov regime, the temperature dependence of the correlation radii describing the decay of  $C_1(\mathbf{r})$  is characterized by two different values of the exponent  $\nu$  ( $\nu = 1/2$  and  $\nu = 1$ ) for the two directions, whereas in the Ising regime the value of  $\nu = 1$  is the same for both directions.

The crossover from the Pokrovsky-Talapov behavior to the Ising one must take place very close to the phase transition temperature, because each point where two DDDWs are created or annihilate is a pair of fractional vortices with topological charges  $q = \pm\frac{1}{4}$  and accordingly has larger energy than a bend on DDDW. It should be emphasized that when the temperature is about 14 times smaller than  $E_B$  even a relatively small increase in energy in comparison with  $E_B$  leads to the suppression of the Boltzmann factor  $\exp(-E_D/T)$  by orders of magnitude.

Just above  $T_{c1}$  the distance between the DDDWs  $L$  is much much larger than their “effective width”  $\xi$  given by the average distance between neighboring bends on a wall,  $\xi \equiv \xi(T) = \exp(E_B/T)$ . Since it is evidently disadvantageous to have  $L \ll \xi$  (this would force the concentration of bends with positive energy to be much larger than the optimal one), the ratio  $L/\xi$  has to saturate with the increase in temperature at  $L/\xi \sim 1$ . For this to take place, the Boltzmann factor

$$w_B(T) \equiv \exp(-E_B/T) \quad (12)$$

has to become much larger than  $f_{DW}/T$ , which allows one to neglect the first term in Eq. (9). Due to the exponential dependence of  $w_B(T)$  on  $T$ , this is achieved at temperatures only slightly above of  $T_{c1}$ .

In this regime the free energy of the fluctuating DDDWs (per lattice plaquette) is of the order of  $-T \exp(-2E_B/T)$ , where one factor  $\exp(-E_B/T)$  is directly related to the energy of the elementary pointlike defect and the other one appears because the distance between neighboring DDDWs has to be exponentially large and, accordingly, the number of places where these pointlike defects can be created is exponentially suppressed. However, in the situation when the fluctuation-induced free energy of domain walls can be neglected (or is absent from the beginning, as in the case of the Berezinskii-Villain interaction), one has to consider also other possibilities for the appearance of pointlike defects in the system. This task is carried out in the next section.



**VI. UNIAXIAL NETWORK STATE**

In this section we, first, discuss what happens at low temperatures if  $f_{DW}$ , the free energy of straight domain walls per unit length, is exactly equal to zero and, therefore, does not induce a removal of the accidental degeneracy of the ground states. And after finding an answer to this question, we return to the problem with small but finite  $f_{DW} > 0$ .

For  $f_{DW} = 0$ , one can expect that at low temperatures a typical configuration, in addition to having parallel straight domain walls, may include a small concentration of local defects (with finite energies) at which these domain walls change their orientations. However, a finite concentration of such objects can appear at arbitrary low temperatures only if the entropy (per defect) of the network of domain walls connecting them can be made arbitrary, large by the decrease of their concentration, as in the gas of noninteracting particles. Without a detailed analysis it is not evident what structure such a network can have and whether its appearance induces a complete disordering of the vortex pattern.

In Sec. IV we have shown that the lowest-energy local defects in our system are pairs of fractional vortices with topological charges  $q = \pm \frac{1}{8}$ . Four different classes of such defects are illustrated in Figs. 3 and 4. However, a network

of domain walls cannot contain the pairs of the type shown in Figs. 3 because the domain walls “emitted” by them can end only on free (that is, unpaired) fractional vortices, which at low temperatures cannot be present in the system.

The neutral pair of fractional vortices shown in Fig. 4(a) is an intersection of single and double domain walls. In order to have a finite concentration of the defects of such a kind, it is necessary to have a sequence of parallel single domain walls and a sequence of double domain walls crossing them. However, the entropy of such a network will be proportional to the number of the walls in these sequences, which does not give the entropic contribution to free energy a chance to overcome the positive term related to the proper energy of the defects and proportional to the number of the intersections. This suggests that such defects cannot play a substantial role in the spontaneous formation of a domain-wall network at the lowest temperatures.

In contrast to that, the neutral fractional-vortex pairs of the two other types shown in Fig. 4(b) and Fig. 4(c) allow for having an arbitrary large entropy per defect. In particular, the configuration shown in Fig. 4(b) is nothing but a bend on a double-spaced double domain wall. In the last paragraph of Sec. V we have argued that for  $f_{DW} \rightarrow 0$  the free energy (per

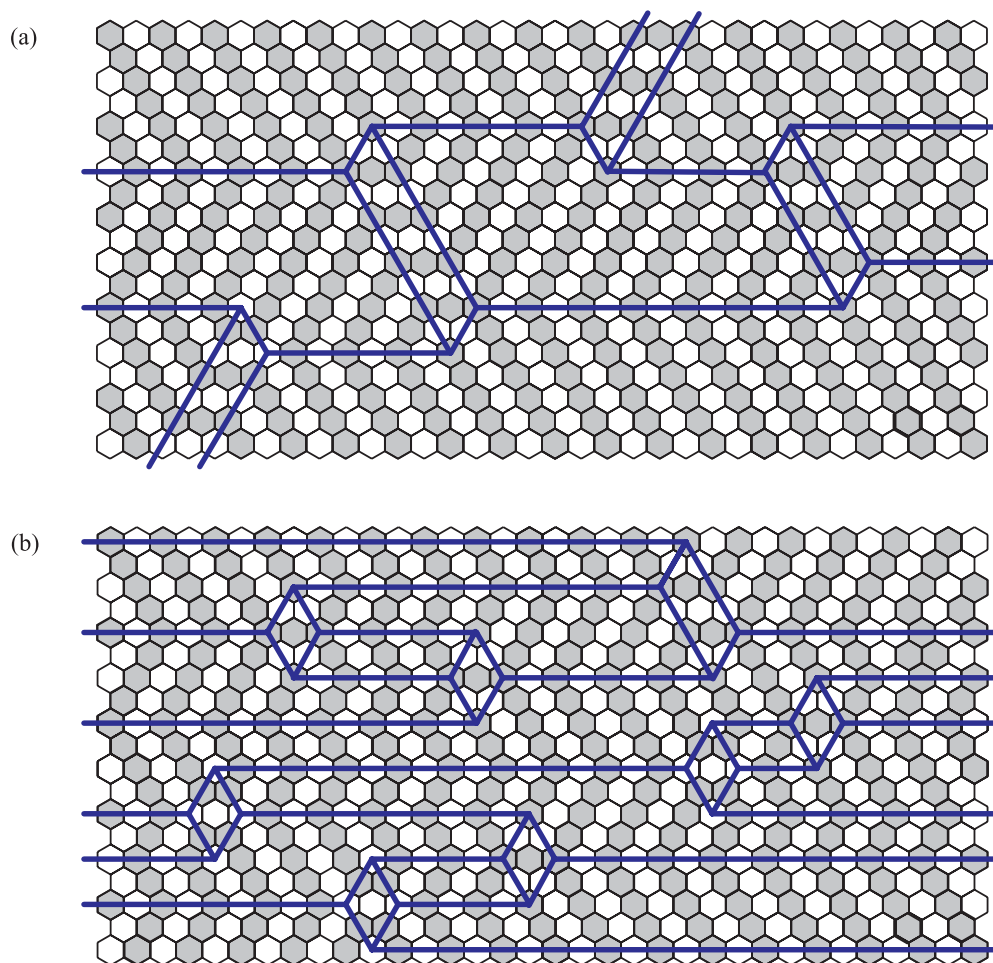


FIG. 7. (Color online) A network formed by parallel single domain walls connected by double-spaced double domain walls: (a) with relatively small density  $n_{DW}$  of single walls; (b) with  $n_{DW} \approx 1/2$ .

site) of the sequence of such double walls has to be of the order of  $-T \exp(-2E_B/T)$ , where  $E_B$  is the energy of a single bend. In this estimate, the exponent contains not just the ratio  $E_B/T$ , like it would if different pointlike defects could be created independently of each other, but  $2E_B/T$ . The second factor  $\exp(-E_B/T)$  appears because double domain walls have to be separated by distances of the order of  $\xi \equiv \exp(E_B/T)$ , and, therefore, the number of places where the pointlike defects with energy  $E_B$  can appear is exponentially suppressed.

Another possibility to get a free energy of comparable order consists in considering configurations in which the energy of pointlike defects is larger than  $E_B$ , but the number of places available for their creation is just proportional to the area of the system without an additional exponential suppression. This happens when one considers a configuration with a finite density  $\rho_{\parallel}$  of parallel single domain walls and inserts into it a finite concentration of pointlike defects, each of which is a double-spaced double domain wall starting on one single wall and ending on a neighboring one, as shown in Fig. 7(a). The energy of these defects is close to  $2E_B$  and, accordingly, for  $\rho_{\parallel} \ll 1$ , the free energy of such a “uniaxial” network can be estimated as

$$F_{\text{UNW}} \sim -\rho_{\parallel} T \exp(-2E_B/T). \quad (13)$$

Note that Fig. 7 gives just a schematic representation of the structure of corresponding states. In reality, at  $T \ll E_B$ , the typical distances between neighboring local defects have to be exponentially large. Accordingly, the mutual influence of the local defects can be neglected.

It is clear from Eq. (13) that it is more profitable to have  $\rho_{\parallel}$  of the order of 1 rather than  $\rho_{\parallel} \ll 1$ . The concentrations close to 1/2 (the average concentration of parallel domain walls in a typical ground state) seem to be the most optimal because they optimize both the number of the available configurations as well as the energy of typical local defects.

The minimum of energy of two fractional-vortex pairs connected by a double-spaced double domain wall is achieved when the four fractional vortices form a symmetric rhombus, as shown in Fig. 8(a). Both for  $V(\theta) = -J \cos \theta$  and for the Berezinskii-Villain interaction, the energy of such a defect,  $E_R$ , is smaller than  $2E_B$  by approximately 11%. The same is true for another defect with the same rhombic arrangement of four fractional vortices shown in Fig. 8(b). Accordingly, the free energy of the domain-wall network containing such defects (and maybe some other defects as well) at the lowest

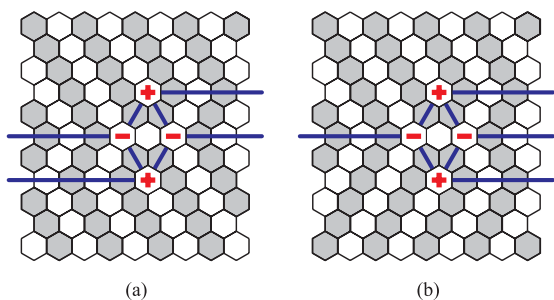


FIG. 8. (Color online) The structure of the typical local defects participating in the formation of the uniaxial network state [shown in Fig. 7(b)].

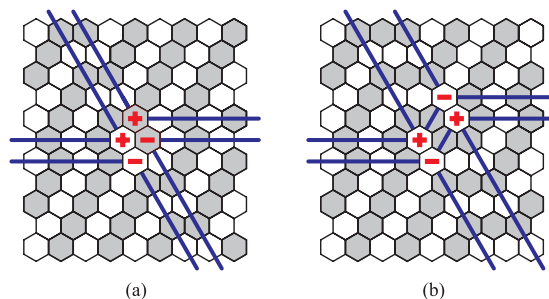


FIG. 9. (Color online) Intersections of double domain walls.

temperatures will be of the order of  $-T \exp(-E_R/T)$ , that is, lower than the free energy of the sequence of fluctuating double walls.

Note that the list of local defects whose energy is lower than  $E_R$ , in addition to configurations that cannot participate in the formation of a domain-wall network (Fig. 3) and bends on double-spaced double domain walls [Fig. 4(b)], includes only the intersections of a double domain wall with either a single wall [Fig. 4(a)] or another double wall (Fig. 9). The presence of such local defects is not sufficient for the construction of a domain-wall network whose entropy dominates over the energy of the defects. This ensures that, for  $f_{\text{DW}} = 0$ , the main role in the formation of the domain-wall network is played by the rhombic defects (shown in Fig. 8) whose presence leads to the formation of the uniaxial network state schematically depicted in Fig. 7(b).

It must be noted that in a typical ground state the concentration of domain walls parallel to each other is equal to 1/2. For  $f_{\text{DW}} = 0$  at the lowest temperatures the system will be in the same phase, the main difference consisting in the presence of an exponentially small concentration of local defects, which shift the positions of domain walls but do not lead to the change of their orientation; see Fig. 7(b). Like at  $T = 0$ , the presence of a finite concentration of parallel domain walls leads to the intermixing of four of six striped vortex patterns. However, there remains a triple degeneracy related to the orientation of domain walls. The order parameter suitable for describing this kind of ordering was introduced in Sec. II B.

In terms of phase correlations, the main qualitative difference with the case of  $T = 0$  is that, at  $T > 0$ , the correlation function  $C_p(\mathbf{r})$  with  $p = 8$  acquires an algebraic decay (analogous correlation functions with  $p < 8$  decay exponentially, even at  $T = 0$ ). However, this property is related not to the appearance of local defects in the domain-wall network but to the presence of spin waves.

Thus, we have found that the formation of local defects works as a mechanism for the removal of the accidental degeneracy of the ground states, which makes the free energy of the system dependent on the concentration of parallel single domain walls  $\rho_{\parallel}$ , with  $F(\rho_{\parallel})$  having the minimum in the vicinity of  $\rho_{\parallel} = 1/2$  (in the limit of  $T \rightarrow 0$  exactly at  $\rho_{\parallel} = 1/2$ ). We now have to remember that in the absence of this mechanism  $F(\rho_{\parallel})$  is equal at small  $\rho_{\parallel}$  to  $f_{\text{DW}}(T)\rho_{\parallel}$  and, accordingly, is minimal at  $\rho_{\parallel} = 0$ . When both mechanisms are taken into account, the function  $F(\rho_{\parallel})$ , at least in some interval of temperatures, will have two minima whose depths change

with temperature. At the temperature where these two depths become equal, a first-order phase transition has to take place.

For  $f_{\text{DW}} > 0$ , a possibility to describe the system assuming  $f_{\text{DW}} = 0$  exists if the ratio

$$\kappa(T) = \frac{f_{\text{DW}}(T)}{T \exp(-E_{\text{R}}/T)} \quad (14)$$

is much smaller than 1. For the model with  $V(\theta) = -J \cos \theta$  the substitution of the expression (8) for  $f_{\text{DW}}(T)$  into Eq. (14) gives that at  $T/J = 0.02$  the value of  $\kappa(T)$  is close to 0.03. Accordingly, at  $T/J \approx 0.02$  the corrections to free energy related to the positiveness of  $f_{\text{DW}}$  can be neglected and one can expect that the free energy of the system is minimal in the uniaxial network state. On the other hand, at  $T/J = 0.015$ , the negative contribution to the free energy related to the appearance of the pointlike defects with energy  $E_{\text{R}}$  cannot overcome the positive term related to the proper free energy of domain walls, and any reasons for the appearance of a uniaxial network with a large concentration of parallel domain walls are absent.

From this it is clear that the first-order transition mentioned above takes place at the temperature  $T_{\text{c}2}$  situated between  $0.015 J$  and  $0.02 J$ . Below this transition the minimum of free energy is achieved in the phase with a sequence of fluctuating double walls described in Sec. V and above it in the uniaxial network with a relatively high density of parallel domain walls. The conclusion that this phase transition is of the first order is additionally confirmed by checking that the presence of fluctuating double-spaced double domain walls does not lead to a decrease of free energy of a single domain wall crossing them. The advantages of the uniaxial domain-wall network manifest themselves only when the density of single domain walls is of the order of  $1/2$ . They consist in the possibility of having local defects of an additional type shown in Fig. 8(b), which increases the number of configurations with the given number of the defects, that is, with the given energy.

## VII. PHASE TRANSITION TO A DISORDERED PHASE

For the complete disordering of vortex pattern the network of domain walls has to have a structure leading to an unbiased mix of all six striped patterns. If all fractional vortices are bound in small neutral pairs, this is impossible. The existence of a finite concentration of such pairs as those shown in Fig. 3 is prohibited by a simple conservation law explained in Sec. IV C, whereas the presence of small concentration of pairs of the three types represented in Fig. 4 leads to the intermixing of only four striped states of six. Such a uniaxial network has a preferable orientation of domain walls.

In order to have an equal representation of all six striped vortex patterns, there should exist a finite concentration of free fractional vortices that are not bound in pairs. If their positions could be arbitrary (that is, not restricted by the requirement for them to be connected by domain walls), free fractional vortices would appear when the two logarithmically divergent contributions to the free energy of a single fractional vortex,

$$F_{\text{FV}} = E_{\text{FV}} - T S_{\text{FV}}, \quad (15)$$

compensate each other. Here,

$$E_{\text{FV}} \approx E_0 \ln L_{\text{max}}, \quad E_0 = \left(\frac{1}{8}\right)^2 \pi \Gamma \quad (16)$$

is the energy of a fractional vortex and  $S_{\text{FV}} \approx 2 \ln L_{\text{max}}$  its entropy, whereas  $\Gamma \equiv \Gamma(T)$  is the helicity modulus<sup>31</sup> and  $L_{\text{max}}$  the size of the system ( $L_{\text{max}} \rightarrow \infty$ ). The prelogarithmic factor in  $F_{\text{FV}}$  becomes equal to zero at  $T = \frac{1}{2} E_0 = \frac{\pi}{128} \Gamma$ . On a honeycomb lattice with the conventional or the Berezinskii-Villain interaction  $\Gamma(T = 0)$  is, respectively, slightly below or slightly above  $J/2$ . Substitution of this value suggests that in the absence of any restrictions related to domain walls free fractional vortices would appear at  $T_{\text{FV}} \approx 0.01 J$ .<sup>32</sup>

Naturally, in the fully frustrated XY model on a honeycomb lattice the entropy of the system of fractional vortices is substantially decreased by the requirement that they have to be connected by straight domain walls (with maybe some rare kinks on them). Moreover, the direction of each domain wall is uniquely determined by the directions of the vortex stripes in the two states that it separates. Nonetheless, these rather strong restrictions still allow for constructing a domain-wall network that leads to an unbiased representation of all six striped vortex patterns. A possible structure of such a network is schematically shown in Fig. 10. Here the letters A, B, and C are used to denote the domains with three different orientations of vortex stripes. Note that all walls between A and B are parallel to each other. The same is true for all walls between B and C, as well as for all walls between C and A. For the sake of lucidity Fig. 10 does not show which of the two versions of A, B, or C (related to the change of the signs of all chiralities) is realized in each particular domain. This depends on the exact positions of domain walls.

Quite remarkably, the entropy (per node) of such a network logarithmically depends on typical distance between neighboring nodes,<sup>26</sup> like it would be in a gas of free particles. This is so because each domain of a network with such a structure can be shifted in parallel to six domain walls that end up in its corners without changing the number of domains or the total length of the domain walls. Thus, if the typical distance between neighboring nodes of the network is of the order of  $L \gg 1$ , then each domain can occupy a number of positions that is proportional to  $L$ . Since the number of domains is equal to one half of the number of nodes, the domain-wall-network entropy per fractional vortex is given (for large-enough  $L$ ) by  $\frac{1}{2} \ln L$  per fractional vortex. This quantity is only 4 times smaller

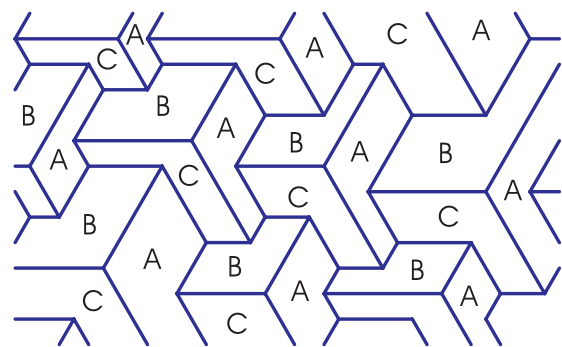


FIG. 10. (Color online) The structure of a domain-wall network in which all six regular vortex pattern are intermixed.

than in the absence of restrictions induced by the presence of domain walls.

The logarithmic behavior of the domain-wall network entropy was first discovered by Villain<sup>33</sup> when considering a honeycomb network in which each domain has the shape of a hexagon with all angles equal to  $120^\circ$ . Such a network is formed in a system with a threefold degeneracy in which a domain wall of a given type (for example, a wall between states A and B) can have only three particular orientations of six that seem to be possible when one looks just at the symmetry of the lattice. A domain-wall network with the structure shown in Fig. 10 (in which each domain also has the shape of a hexagon but with angles of  $60^\circ$ ,  $120^\circ$ , and  $240^\circ$ ) has been proposed for the Ising model on a triangular lattice with the antiferromagnetic interaction of the nearest and second and third neighbors.<sup>26</sup> For some relation between parameters, the ground states of this Ising model have the striped structure<sup>25</sup> completely analogous to that of the striped ground states of the considered XY model. However, the important difference between the two models is that in the model we discuss now the nodes of the domain-wall network have a long-range logarithmical interaction.

In accordance with that, in the fully frustrated XY model on a honeycomb lattice the free energy (per lattice plaquette) of a domain-wall network with the structure shown in Fig. 10 is given by

$$F_{\text{NW}} = \frac{c_1}{L^2} \left( E_0 - \frac{T}{2} \right) \ln L + F_{\text{NW}}^{(1)}(L), \quad (17)$$

where  $c_1 \sim 1$  is a constant of purely geometrical origin, whereas  $L \gg 1$  is the typical distance between neighboring fractional vortices. The last term in Eq. (17) describes the dominant corrections to the logarithmic terms and for  $L \gg 1$  can be estimated as  $F_{\text{NW}}^{(1)}(L) \sim E_0/L^2$ .

At  $T < T_{\text{FV}} = 2E_0$ , when both terms in Eq. (17) are positive, the minimum of  $F_{\text{NW}}$  is achieved when  $L \rightarrow \infty$ , that is, in the absence of a domain-wall network. On the other hand, at  $T > T_{\text{FV}}$  the free energy of the system at large  $L$  decreases with the decrease in  $L$ . Therefore, the optimal value of  $L$  at such temperatures is determined by the interplay between the two terms in Eq. (17). It is then clear, without performing any calculations, that when  $T$  tends to  $T_{\text{FV}}$  from above, the value of  $L$  minimizing  $F_{\text{NW}}$  goes to infinity.

However, all the conclusions of the previous paragraph would be applicable only if any other fluctuations save the formation of a domain-wall network with the structure shown in Fig. 10 are prohibited. In reality, one expects that at such temperatures the system is in the uniaxial-network state with a large concentration of parallel domain walls. In this situation, the structure of the domain-wall network related to the appearance of unpaired fractional vortices also can be illustrated by Fig. 10, where now the domains denoted by the same letter correspond to uniaxial-network states with the same dominant orientation of domain walls. Nonetheless, exactly as before, each node of the network corresponds to an unpaired fractional vortex with topological charge  $q = \pm \frac{1}{8}$ , which means that one can still use Eq. (17) for describing the energy of the interaction of unpaired fractional vortices plus the entropy of the network related to fluctuations of positions

of different domains. However, one also has to add to this expression the energy of the boundaries between different uniaxial networks.

A boundary between two uniaxial-network states with different preferable orientations of domain walls is schematically shown in Fig. 11, where each line corresponds to a domain wall, whereas letters A, B, and C again denote domains with three different orientations of vortex stripes. Note that one of the uniaxial networks (the one to the right) contains mainly domains A and C, whereas the other one domains B and C. It is clear that the change of the dominant orientation of domain walls that has to take place at a boundary between domains requires to have a large concentration of fractional vortices on this boundary and, accordingly, the energy of such a boundary per unit length has to be of the order of  $E_0$ .

Accordingly, the expression for the free energy of the domain-wall network formed by unpaired fractional vortices separated by distances of the order of  $L$  must also contain a positive contribution of the order of  $E_0/L$ , which, for large  $L$ , will always dominate over the first term in Eq. (17). This suggests that the phase transition related to the appearance of free fractional vortices must take place at  $T = T_{c3} > T_{\text{FV}}$  and has to be of the first order, because the two minima of the function  $F_{\text{NW}}(L)$  (at  $L = \infty$  and at finite  $L$ ) will always be separated by some barrier. Moreover, since the behavior of the function  $F_{\text{NW}}(L)$  is determined (in addition to  $T$ ) by the single energy scale,  $E_0$ , one can expect that the shift of the transition temperature,  $T_{c3}$ , with respect to  $T_{\text{FV}}$  will be of the order of  $E_0$ , whereas the typical distance between fractional vortices just above the transition can be only numerically larger than 1, and not parametrically. Accordingly, we can conclude that  $T_{c3} \sim (0.05 \div 0.1)J$  but cannot provide a more accurate estimate.

Note that the formation of a domain-wall network leading to the intermixing of all six striped vortex patterns is impossible without the proliferation of free fractional vortices. This means that there is no possibility for the phase transitions related with the removal of the triple degeneracy of the uniaxial network states and suppression of the algebraic phase behavior of  $C_8(\mathbf{r})$  to take place at different temperatures. On the other hand, the

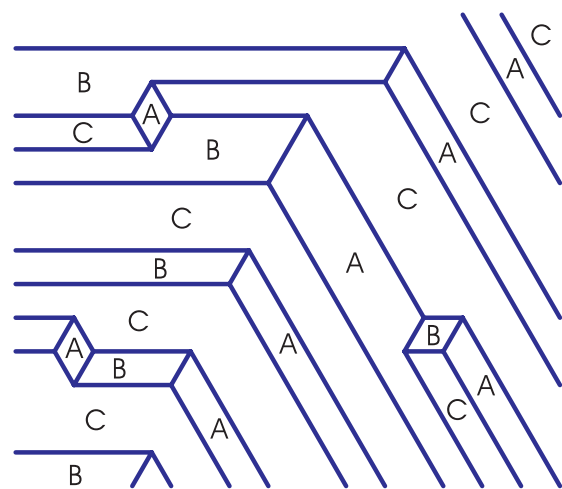


FIG. 11. (Color online) A boundary between two uniaxial networks with different preferable orientations of domain walls.



appearance of free fractional vortices leads to the screening of the logarithmic interaction of the conventional vortices, so the pairs of such vortices also unbind. Accordingly, at  $T > T_{c3}$ , the system is in the completely disordered phase in which all correlations decay exponentially.

### VIII. CONCLUSION

#### A. Phase diagram

The main results of this work are summarized in Table I, which reviews the properties of various phases represented in the phase diagram of the fully frustrated XY model on a honeycomb lattice. The order in which these phases are listed corresponds to the increase in temperature. By the existence of the long-range order (LRO) in terms of vortex pattern, we mean the selection of one of the six equivalent striped vortex patterns; see Fig. 1(a). On the other hand, the existence of the long-range order in terms of the domain-wall orientation implies the choice of one of the three preferable orientations of domain walls. The last three columns describe the behavior of the gauge-invariant phase correlation functions defined by Eq. (7).

The first line in Table I refers to the behavior of the correlation functions when the averages are calculated over the set of the all ground states of the model. A typical ground state incorporates an irregular sequence of parallel straight domain walls, which leads to the exponential decay of the chirality correlation function, Eq. (4), as well as of phase correlation functions  $C_p(\mathbf{r})$  with  $p < 8$  for all directions that are not exactly perpendicular to one of the directions of lattice bonds. Nonetheless, the system has the long-range order in terms of domain-wall orientation.

At  $T > 0$  domain walls acquire a finite free energy per unit length given by Eq. (8) and originating from the difference in the free energy of spin waves.<sup>14</sup> At the lowest temperatures, this leads to the suppression of infinite domain walls crossing the whole system and the appearance of the long-range order in terms of vortex pattern (phase No. 1 in Table I). The system spontaneously chooses one of the six equivalent striped vortex patterns. On the other hand, all phase correlation functions decay algebraically due to the presence of spin waves.

With the increase in temperature, the first phase transition takes place at  $T = T_{c1} \approx 0.8 \times 10^{-2} J$  and is related to the appearance of a sequence of fluctuating double-spaced double domain walls. On average, the direction of these fluctuating walls is perpendicular to the direction of the vortex stripes. This

phase transition is continuous with the Ising-type behavior in a very narrow critical region and the Pokrovsky-Talapov behavior in a wider region around the critical one. Although the transition taking place at  $T = T_{c1}$  is related to the appearance of domain walls, above it (phase No. 2 in Table I) the discrete degeneracy (related to the long-range order in terms of vortex pattern) remains the same (sixfold), whereas the decay of the phase correlation function  $C_1(\mathbf{r})$  changes from algebraic to exponential. This happens because the presence of a doubly spaced double domain wall between two points shifts the phase difference by  $\pi$ .

The next phase that appears with the increase in temperature (phase No. 3 in Table I) has the same symmetry properties as a typical ground state of the model. In particular, in this phase there is no long-range order in terms of vortex pattern. The main difference with a random sequence of parallel straight domain walls (characteristic for a typical ground state) consists in the presence of local defects which shift the positions of these walls but do not change their preferable orientation; see Fig. 7(b). The phase transition to this uniaxial domain-wall network has to be of the first order and can be expected to take place at  $T = T_{c2} \sim 2T_{c1}$ .

The important feature of the uniaxial domain-wall network is that the nodes of this network, which, in terms of phase variables, correspond to logarithmically interacting fractional vortices, are bound in neutral pairs. As a consequence of this, the helicity modulus in this phase is finite, like in the other ordered phases discussed above. Since all three ordered phases have some preferred direction (of vortex stripes or of domain walls), the helicity modulus in all of them has to be anisotropic.

The phase transition to the disordered phase (phase No. 4 in Table I) with the complete suppression of the long-range order and exponential decay of all correlation functions can be associated with the appearance of an isotropic domain-wall network in which some fractional vortices (the nodes of the network) are not bound in pairs but are free. By analyzing how the free energy of such a network depends on typical distance between free fractional vortices, it is possible to establish that this transition must be of the first order and has to occur at  $T_{c3} \sim (0.05 \div 0.1)J$ .

All phase transitions mentioned above take place at temperatures that are much lower than the temperature  $T_{\text{BKT}} \sim J$  at which the unbinding of pairs of the conventional vortices (with integer topological charges) would take place if any other fluctuations were absent. At  $T \ll T_{\text{BKT}}$ , the presence of an exponentially small concentration of small bound pairs of

TABLE I. The properties of different phases of the fully frustrated XY model on a honeycomb lattice; “exp” denotes an exponential decay of the corresponding correlation function (for a generic direction) and “a” an algebraic decay.

No.	Temperature interval	Domain wall presence	LRO in terms of		Decay of phase correlation functions		
			Vortex pattern	Domain wall orientation	$C_1(\mathbf{r})$	$C_2(\mathbf{r})$	$C_8(\mathbf{r})$
	$T = 0$	Straight parallel domain walls	—	+	exp	exp	LRO
1	$0 < T < T_{c1}$	No infinite domain walls	+	—	a	a	a
2	$T_{c1} < T < T_{c2}$	Sequence of fluctuating DDDWs	+	—	exp	a	a
3	$T_{c2} < T < T_{c3}$	Uniaxial domain-wall network	—	+	exp	exp	a
4	$T_{c3} < T$	Isotropic domain-wall network	—	—	exp	exp	exp

integer vortices does not lead to any noticeable consequences and, therefore, can be neglected. On the other hand, at  $T > T_{c3}$ , the logarithmic interaction of integer vortices is screened due to the presence of a finite concentration of free fractional vortices and, therefore, there are no grounds to expect the existence of an additional phase transition related to the unbinding of integer vortices.

### B. Discussion

Thus, we have established that the equilibrium thermodynamics of the fully frustrated  $XY$  model on a honeycomb lattice supports the existence at  $T > 0$  of four different phases, three of which are characterized by the presence of a long-range order. However, the observation of some of these phases (and the phase transitions between them) in a real or numerical experiment may turn out to be a big problem.

In particular, at  $0 < T < T_{c1}$ , the complete suppression of domain walls crossing the whole system (induced by the spin-wave contribution to their free energy, see Sec. III) is achieved only in the thermodynamic limit,  $L_{\max} \rightarrow \infty$ . In a finite system with linear size  $L_{\max}$ , in order to have the average number of such walls smaller than 1, the size of the system should be larger than  $L_c(T)$ , the temperature-dependent solution of the equation

$$L_{\max} \exp\left(-\gamma \frac{TL_{\max}}{J}\right) = 1. \quad (18)$$

At  $T = T_{c1}$ , the point of the phase transition related to the appearance of infinite double-spaced double domain walls,  $L_c \approx 3 \times 10^7$ . This means that numerical simulations of systems with  $L \lesssim 10^7$  does not allow one to observe the phase with suppressed domain walls independently of whether it is possible to reach the thermal equilibrium at  $T \sim T_{c1}$ .

More or less the same criterion applies to the observation of the phase with a sequence of fluctuating double domain walls. Accordingly, for  $L \lesssim 10^7$  the increase of temperature will lead just to a smooth crossover from a random sequence of parallel straight domain walls to the uniaxial domain-wall network with the same preferable orientations of domain walls. However, a discontinuous transition from the uniaxial domain-wall network to an isotropic one (the disordered phase) can be expected to be observable, even if the size of the system is not so large. On the other hand, it follows from the numerical simulations of Refs. 17 and 18 that the task of reaching thermal equilibrium at  $T \lesssim 0.1 J$  will require very special effort for its implementation. Moreover, the phase with a uniaxial domain-wall network cannot be observed by the methods<sup>18</sup> assuming the existence of the long-range order in terms of the vortex pattern. Instead, one should look for the anisotropy of a current distribution or for the appearance of a finite helicity modulus (superfluid density).

In the case of the Berezinskii-Villain interaction, the free energy of spin waves is exactly the same for all domain-wall configurations and, therefore, does not lead to the removal of the accidental degeneracy of the ground states. In such a situation, a smooth crossover from a random sequence of parallel straight domain walls to the uniaxial domain-wall network is realized not only when  $L_{\max} \lesssim L_c$  but also in the thermodynamic limit. That is, instead of three phase

transitions, an infinite system with the Berezinskii-Villain interaction must experience only one, related to the loss of the long-range order in the orientation of domain walls and of the algebraic decay of  $C_8(\mathbf{r})$ . The conclusion that this transition has to be of the first order is not sensitive to a particular form of the interaction in the Hamiltonian of the model.

Since the fully frustrated  $XY$  model with the Berezinskii-Villain interaction on a honeycomb lattice is exactly equivalent to the half-integer Coulomb gas on a triangular lattice, the scenario described in the previous paragraph has to be realized also in such a Coulomb gas. Numerical simulations of the half-integer Coulomb gas on a triangular lattice were undertaken by Lee and Teitel,<sup>15</sup> who have discovered a relatively sharp jump of the dielectric function at  $T/J \sim 0.04$  but assumed it to be a finite-size-induced artifact. This conclusion was based on the observation that the formation and motion of finite-energy local defects (analogous to those shown in our Fig. 8) destroys the long-range order in the vortex pattern at an arbitrary low temperature. However, this argument missed the possibility of having the long-range order in the domain-walls orientation, which, according to our analysis, should be present in the half-integer Coulomb gas on a triangular lattice at low-enough temperatures.

It should be mentioned that a uniformly frustrated  $XY$  model with this or that interaction provides just an idealized description of a Josephson junction array or of a superconducting wire network. In physical situations there can exist other mechanisms for the removal of the accidental degeneracy of the ground states related to the interactions not taken into account in the framework of an  $XY$  model. One of them is the magnetic interaction of currents in the junctions or in the wires. However, it is likely that the sign of the domain-wall energy induced by this interaction may depend on the particular geometry of the system.

If  $E_{DW}$ , the domain-wall energy per unit length, is positive, this will substantially improve the possibilities for the observation of the phase with the striped vortex pattern. Even if  $E_{DW}$  is a few orders of magnitude smaller than  $J$ , it will be many orders of magnitude larger than the value of  $f_{DW}$  given by Eq. (8) at the corresponding temperatures. The opposite sign of  $E_{DW}$  will lead to the stabilization of another periodic vortex pattern shown in Fig. 1(c) of Ref. 14. In any case, a nonzero value of  $E_{DW}$  will allow the observation of a phase with a long-range order in terms of vortex pattern in the systems of less than macroscopic sizes.

On the other hand, the magnetic interaction of currents leads to the screening of the logarithmic interaction of vortices (both conventional and fractional) at large distances. This will transform the phase transition related to the appearance of a sequence of fluctuating double-spaced double domain walls into a crossover, because when the logarithmic interaction of fractional vortices is screened, such double walls no longer are topologically stable defects and can have free end points. A substantial increase of  $E_{DW}$  may lead also to the disappearance of the region of stability of the uniaxial network state, which implies a direct transition from the phase with the long-range order in terms of vortex pattern into the disordered phase.

Another mechanism for the stabilization of striped vortex patterns in magnetically frustrated superconducting wire networks may be related with the nonuniformity of the

order parameter amplitude<sup>34</sup> (see also Ref. 35). However, the conclusions of Ref. 34 are in some contradiction with the results of Ref. 36 devoted to including into analysis the higher-order terms of the Ginzburg-Landau expansion, which suggests that the problem requires further investigation.

The uniformly frustrated  $XY$  model with triangular lattice and  $f = \frac{1}{4}$  also allows for the formation of zero-energy domain walls parallel to each other,<sup>23</sup> so its phase diagram may have some common features with the one constructed in this work. In the uniformly frustrated  $XY$  model with  $f = \frac{1}{3}$  on a triangular lattice,<sup>23</sup> as well as in the fully frustrated  $XY$  model on a dice lattice,<sup>37,38</sup> the situation is more complex because these models allow for the formation of two sets of parallel zero-energy domain walls that can cross each other without paying any energy for this. However, in such a situation, it is also possible to expect the existence of a phase in which vortex pattern is disordered, whereas the long-range order is related to the orientation of domain walls.

On the experimental side, the conclusions of this work may be applicable not only to Josephson junction arrays and superconducting wire networks with a half-integer number of flux quanta per plaquette but also to magnetically frustrated triangular arrays of microholes<sup>39</sup> or nanoholes<sup>40</sup> in thin superconducting films. For a half-integer number of flux quanta per hole, the energy of different vortex configurations in such objects has to be described by the Hamiltonian of the half-integer Coulomb gas with screened logarithmic interaction.

The most reliable approaches to the experimental identification of the phase with the long-range order in terms of vortex pattern may be based on the methods involving direct observation of vortex arrangement by monitoring the magnetic field distribution. This phase is also characterized by the anisotropic superfluid density. In the phase with the uniaxial domain network the superfluid density is also anisotropic, but the long-range order in terms of the vortex pattern is absent.

#### APPENDIX A: BEREZINSKII-VILLAIN INTERACTION AND THE COULOMB GAS REPRESENTATION

A magnetically frustrated network formed by identical superconducting wires can be described in the London regime (when the amplitude of the superconducting order parameter is uniform along the wires) by the Hamiltonian<sup>41</sup>

$$H = \frac{J}{2} \sum_{(jj')} \theta_{jj'}^2, \quad (\text{A1a})$$

where  $\theta_{jj'}$  is the integral of the gauge-invariant phase gradient along the wire connecting nodes  $j$  and  $j'$ . Variables  $\theta_{jj'}$  can acquire arbitrary values,  $-\infty < \theta_{jj'} < +\infty$ , but on any plaquette of the lattice have to satisfy the constraint

$$\sum_{\square\alpha} \theta_{jj'} = -2\pi f \pmod{2\pi}, \quad (\text{A1b})$$

where parameter  $f$  depends on the applied magnetic field and is equal to the number of superconducting flux quanta per plaquette.

In terms of phase variables  $\varphi_j$  defined on the nodes of the network, the partition function of the model (A1) can be

rewritten<sup>42</sup> as the partition function of the uniformly frustrated  $XY$  model with the so-called Berezinskii-Villain interaction  $V_{\text{BV}}(\theta)$  defined by the relation

$$\exp\left[-\frac{V_{\text{BV}}(\theta)}{T}\right] = \sum_{h=-\infty}^{\infty} \exp\left[-\frac{J}{2T}(\theta - 2\pi h)^2\right]. \quad (\text{A2})$$

The function  $V_{\text{BV}}(\theta)$  has the same symmetry and periodicity as  $V(\theta) = -J \cos \theta$ . For  $J \gg T$  it is everywhere except the close vicinity of the point  $\theta = \pi$  close to parabola,  $V_{\text{BV}}(\theta) \approx (J/2)\theta^2 + \text{const}$ . In the opposite limit,  $J \ll T$ , the function  $V_{\text{BV}}(\theta)$  with an exponential accuracy is reduced to  $-J_{\text{eff}} \cos \theta + \text{const}$ , where, however, the coupling constant  $J_{\text{eff}} = 2T \exp(-T/2J)$  is much smaller than  $J$ .

The interaction function defined by Eq. (A2) was introduced by Berezinskii<sup>7</sup> and Villain<sup>8</sup> because it allows one to simplify the analytical analysis of  $XY$  models. The integration over variables  $\varphi_j$  in the partition function of an  $XY$  model with such an interaction is Gaussian and, therefore, can be performed exactly. In particular, in the case of the periodic boundary conditions the application of this procedure transforms the partition function of a uniformly frustrated  $XY$  model with the Berezinskii-Villain interaction into that of a ‘‘fractional’’ Coulomb gas<sup>9</sup> described by the Hamiltonian

$$H_{\text{CG}} = \frac{1}{2} \sum_{\alpha,\beta} m_\alpha G_{\alpha\beta} m_\beta, \quad (\text{A3})$$

where variables  $m_\alpha$  (the charges of the Coulomb gas) are defined on the sites  $\alpha$  of the dual lattice and acquire values shifted with respect to integers by  $-f$ . Each of these variables is proportional to the sum of variables  $\theta_{jj'} - h_{jj'}$  (defined on lattice bonds) over the perimeter of plaquette  $\alpha$  and, in terms of the  $XY$  representation, can be identified with the vorticity of this plaquette divided by  $2\pi$ .

The long-range interaction  $G_{\alpha\beta}$  entering Eq. (A3) has a form,

$$G_{\alpha\beta} = 4\pi^2 J (-\hat{\Delta})_{\alpha\beta}^{-1}, \quad (\text{A4})$$

where  $\hat{\Delta}$  is the discrete Laplace operator on the dual lattice. This interaction logarithmically depends on  $r_{\alpha\beta} = |\mathbf{r}_\alpha - \mathbf{r}_\beta|$ , the distance between  $\alpha$  and  $\beta$ ,

$$G_{\alpha\alpha} - G_{\alpha\beta} = 2\pi \Gamma_0 (\ln r_{\alpha\beta} + \kappa), \quad (\text{A5})$$

where  $\Gamma_0$  is proportional to  $J$  but also depends on the structure of the lattice. In terms of the  $XY$  representation  $\Gamma_0$  is the helicity modulus describing the rigidity of the system with respect to phase twist. In the considered case  $\Gamma_0 = J/\sqrt{3}$ , whereas  $\kappa = \pi/\sqrt{3}$  for  $r_{\alpha\beta} = 1$  (the nearest neighbors on the triangular lattice) and monotonically increases by less than 0.5% with the increase of  $r_{\alpha\beta}$  to infinity.

It can be expected that the number of qualitative features of frustrated  $XY$  models with the conventional and with the Berezinskii-Villain interactions are the same. However, in situations when the ground states of the model possess an accidental degeneracy, one should be cautious because, in a model with the Berezinskii-Villain interaction, the free energy of the spin waves is exactly the same for all vortex configurations and, therefore, does not lead to the removal of such a degeneracy (in contrast to the models with the conventional form of the interaction).

In the case of a fully frustrated model (with  $f = \frac{1}{2}$ ), the charges of the Coulomb gas are half-integer. Since the charges of the opposite signs attract each other, it is rather clear that when the dual lattice is bipartite (square or honeycomb), the minimum of energy is achieved in configurations with a regular (checkerboard-like) alternation of positive and negative charges. This is in a perfect agreement with having a twofold discrete degeneracy of the ground states in terms of the  $XY$  representation. In the case of the half-integer Coulomb gas on a triangular lattice it is impossible to construct a configuration in which each charge has neighbors only of the opposite sign. Accordingly, it is much less evident what are the states minimizing the energy and how high is their degeneracy. In Appendix B we propose a transformation that substantially simplifies this task and also provides a transparent expression for the energies of the excited states of the half-integer Coulomb gas.

### APPENDIX B: EFFECTIVE CHARGE REPRESENTATION

When considering the half-integer Coulomb gas described by Hamiltonian (A3), it is convenient to introduce auxiliary variables  $q_\alpha$  linearly related to  $m_\alpha$ ,

$$q_\alpha = m_\alpha + \lambda \hat{\Delta}_{\alpha\beta} m_\beta, \quad (\text{B1})$$

where  $\hat{\Delta}_{\alpha\beta}$  is the discrete Laplacian on the lattice on which variables  $m_\alpha$  are defined and the choice of  $\lambda$  depends on the structure of this lattice. The replacement of  $m_\alpha$  by  $q_\alpha - \lambda \hat{\Delta}_{\alpha\beta} m_\beta$  allows one to rewrite Eq. (A3) as

$$H_{\text{CG}} = \frac{1}{2} \sum_{\alpha,\beta} q_\alpha G_{\alpha\beta} q_\beta + 4\pi^2 J (\lambda - \lambda^2 z) \sum_{\alpha} m_\alpha^2 + 2\pi^2 J \lambda^2 \sum_{(\alpha\alpha')} (m_\alpha + m_{\alpha'})^2, \quad (\text{B2})$$

where  $z$  is the coordination number of the lattice, whereas the summation in the last term is performed over all pairs of nearest neighbors ( $\alpha\alpha'$ ). The form of Eq. (B2) suggests that the long-range interaction of the charges of the half-integer Coulomb gas can be replaced by their repulsion on neighboring sites plus the long-range interaction of the ‘‘effective charges’’  $q_\alpha$  defined by Eq. (B1). Naturally, it is convenient to choose the value of  $\lambda$  in such a way that, in the ground states, all effective charges are equal to zero, which substantially simplifies the calculation of energy and also minimizes the first term in Eq. (B2).

For  $\lambda < 1/z$  the second term in Eq. (B2) is minimized when  $m_\alpha = \pm \frac{1}{2}$ , whereas the third term requires maximization of the number of bonds on which  $m_\alpha$  and  $m_{\alpha'}$  have opposite signs. On bipartite lattices it is always possible to do this for any pair of neighboring sites. In such a case, the fulfillment of condition  $q_\alpha = 0$  is achieved when one takes  $\lambda = 1/(2z)$ . For a square lattice this gives  $\lambda = \frac{1}{8}$  and for a honeycomb lattice  $\lambda = \frac{1}{6}$ . For these values of  $\lambda$  the states with the regular checkerboard alternation of positive and negative charges  $m_\alpha = \pm \frac{1}{2}$  ensure the simultaneous minimization of all three terms in Eq. (B2), which rigorously proves that they are the ground states.

In the case of a triangular lattice, each plaquette has to have either one or three bonds with the same sign of  $m_\alpha$  and  $m_{\alpha'}$ . As a consequence of this, on average, each charge has to have at least two neighbors of the same sign. In such a situation it

is convenient to take  $\lambda = \frac{1}{8}$ , which for all configurations with  $m_\alpha = \pm \frac{1}{2}$  reduces Eq. (B2) to

$$H_{\text{CG}} = \frac{1}{2} \sum_{\alpha,\beta} q_\alpha G_{\alpha\beta} q_\beta + \left( N + \frac{N_3}{2} \right) g, \quad (\text{B3})$$

where

$$g = \left( \frac{\pi}{4} \right)^2 J, \quad (\text{B4})$$

$N$  is the total number of sites, and  $N_3$  is the number of triangular plaquettes on which all three charges have the same signs. It is evident that the first term in Eq. (B3) is minimized when all variables  $q_\alpha$  are equal to zero and the second one when  $N_3 = 0$ . Since both these conditions can be fulfilled simultaneously, constant  $g$  is nothing else but the ground-state energy per site. Note that the value of  $g$  given by Eq. (B4) is in perfect agreement with having, in the fully frustrated  $XY$  model,  $\theta_{jj'} = 0$  on one-third of the bonds of the honeycomb lattice and  $\theta_{jj'} = \pm\pi/4$  on all other bonds.

Thus, the set of the ground states of the half-integer Coulomb gas includes all states in which all charges are equal to  $\pm 1/2$ , each charge has exactly two neighbors of the same sign, and, on each triangular plaquette, there are always two charges of one sign and one charge of the opposite sign. These states can be put into the correspondence with the ground states of the fully frustrated  $XY$  model on a honeycomb lattice by interpreting the charges  $m_\alpha$  as vorticities (divided by  $2\pi$ ) of the corresponding plaquettes, as it could be expected from the equivalence between the half-integer Coulomb gas and the fully frustrated  $XY$  model with the Berezinskii-Villain interaction on the dual lattice (see Appendix A). However, the reduction of Hamiltonian (A3) to the form (B3) has allowed us to find the structure of the ground states of the half-integer Coulomb gas on a triangular lattice directly in terms of the Coulomb gas representation.

Note that the form of Eqs. (B2) and (B3) relies on the very special form of the interaction of charges in the Coulomb gas [given by Eq. (A4)]. As soon as the form of the interaction is modified (for example, to take into account the screening effects in a superconducting array or wire network), the possibility to transform the Hamiltonian to the form of Eq. (B2) with only local interaction of variables  $m_\alpha$  disappears, which leads to a partial removal of the degeneracy between the states with  $q_\alpha = 0$  and  $N_3 = 0$ .

TABLE II. The energies (in units of  $J$ ) of the finite-energy defects presented in Figs. 3–9 in the case of the Berezinskii-Villain interaction.

Figure number	Defect energy	Notation
3(a)	0.102808	
3(b)	0.134471	
4(a), 4(b), 4(c)	0.142292	$E_B$
9(b)	0.197419	
9(a)	0.237279	
8(a), 8(b)	0.253298	$E_R$
6(b)	0.347909	
5(a)	0.371750	$E_K$
5(c)	1.977200	$E_K^s$



In the configurations with  $m_\alpha = \pm\frac{1}{2}$  on a triangular lattice, the values of effective charges  $q_\alpha$  are given by

$$q_\alpha = \frac{N_\alpha - 2}{4} m_\alpha, \quad (\text{B5})$$

where  $N_\alpha$  is the number of the nearest neighbors of site  $\alpha$  with the same sign of the charge  $m$ . It follows from Eq. (B5) that the effective charges of various sites are either zero or equal to  $\pm\frac{1}{8}$  or multiples of these values. In Sec. IV B, the appearance of logarithmically interacting vortices with fractional topological charges on those plaquettes of the honeycomb lattice which

have the number of neighbors with the same sign of vorticity not equal to two has been discussed directly in terms of the XY model.

Equation (B3) provides a convenient way for calculating the energies of local defects in half-integer Coulomb gas on a triangular lattice (or in the equivalent fully frustrated XY model with the Berezinskii-Villain interaction on a honeycomb lattice) by summing just few terms. The values of these energies for various finite-energy defects discussed above and illustrated in Figs. 3–9 are listed in Table II.

- <sup>1</sup>S. Teitel and C. Jayaprakash, *Phys. Rev. Lett.* **51**, 1999 (1983).  
<sup>2</sup>M. Hasenbusch, A. Pelissetto, and E. Vicari, *J. Stat. Mech.: Th. Exp.* P12002 (2005).  
<sup>3</sup>S. E. Korshunov, *Usp. Fiz. Nauk* **176**, 233 (2006); *Phys. Usp.* **49**, 225 (2006).  
<sup>4</sup>For reviews, see R. S. Newrock, C. J. Lobb, U. Geigenmüller, and M. Octavio in *Solid State Physics*, Vol. 54, edited by H. Ehrenreich and F. Spaepen (Academic Press, San Diego, 2000), p. 263; P. Martinoli and Ch. Leemann, *J. Low Temp. Phys.* **118**, 699 (2000).  
<sup>5</sup>J. Villain, *J. Phys. C* **10**, 1717 (1977).  
<sup>6</sup>L. B. Ioffe and M. V. Feigel'man, *Phys. Rev. B* **66**, 224503 (2002); B. Douçot, M. V. Feigel'man, and L. B. Ioffe, *Phys. Rev. Lett.* **90**, 107003 (2003).  
<sup>7</sup>V. L. Berezinskii, Ph.D. thesis, L. D. Landau Institute, 1971, published by Fizmatlit, Moscow, 2007 (in Russian).  
<sup>8</sup>J. Villain, *J. Phys. (Paris)* **36**, 581 (1975).  
<sup>9</sup>E. Fradkin, B. A. Huberman, and S. H. Shenker, *Phys. Rev. B* **18**, 4789 (1978).  
<sup>10</sup>S. E. Korshunov, *Phys. Rev. Lett.* **88**, 167007 (2002).  
<sup>11</sup>P. Olsson, *Phys. Rev. B* **55**, 3585 (1997).  
<sup>12</sup>W. Y. Shih and D. Stroud, *Phys. Rev. B* **32**, 158 (1985).  
<sup>13</sup>S. E. Korshunov, *J. Stat. Phys.* **43**, 17 (1986).  
<sup>14</sup>S. E. Korshunov and B. Douçot, *Phys. Rev. Lett.* **93**, 097003 (2004).  
<sup>15</sup>J.-R. Lee and S. Teitel, *Phys. Rev. B* **46**, 3247 (1992).  
<sup>16</sup>W. Y. Shih and D. Stroud, *Phys. Rev. B* **30**, 6774 (1984).  
<sup>17</sup>R. W. Reid, S. K. Bose, and B. Mitrović, *J. Phys.: Condens. Matter* **9**, 7141 (1997).  
<sup>18</sup>E. Granato, *Phys. Rev. B* **85**, 054508 (2012).  
<sup>19</sup>R. N. Bhatt and A. P. Young, *Phys. Rev. B* **37**, 5606 (1988).  
<sup>20</sup>J. Villain, R. Bidaux, J. P. Carton, and R. Conte, *J. Phys. (France)* **41**, 1263 (1980).  
<sup>21</sup>E. F. Shender, *Zh. Eksp. Teor. Fiz.* **83**, 326 (1982) [*Sov. Phys. JETP* **56**, 178 (1982)].  
<sup>22</sup>H. Kawamura, *J. Phys. Soc. Jpn.* **53**, 2452 (1984); S. E. Korshunov, *Pis'ma Zh. Eksp. Teor. Fiz.* **41**, 525 (1985) [*JETP Lett.* **41**, 641 (1985)]; *J. Phys. C* **19**, 5927 (1986); C. L. Henley, *J. Appl. Phys.* **61**, 3962 (1987); *Phys. Rev. Lett.* **62**, 2056 (1989).  
<sup>23</sup>S. E. Korshunov, A. Vallat, and H. Beck, *Phys. Rev. B* **51**, 3071 (1995).  
<sup>24</sup>Analogous hidden symmetry exists also in the fully frustrated XY model on a dice lattice, see Ref. 37.  
<sup>25</sup>B. D. Metcalf, *Phys. Lett. A* **46**, 325 (1974); M. Kaburagi and J. Kanamori, *Jpn. J. Appl. Phys.* **13**, Suppl. 2-2, 145 (1974).  
<sup>26</sup>S. E. Korshunov, *Phys. Rev. B* **72**, 144417 (2005).  
<sup>27</sup>T. C. Halsey, *J. Phys. C* **18**, 2437 (1985); S. E. Korshunov and G. V. Uimin, *J. Stat. Phys.* **43**, 1 (1986).  
<sup>28</sup>S. E. Korshunov, *Pis'ma Zh. Eksp. Teor. Fiz.* **41**, 216 (1985) [*Sov. Phys.- JETP Lett.* **41**, 263 (1985)]; *J. Phys. C* **19**, 4427 (1986); D. H. Lee and G. Grinstein, *Phys. Rev. Lett.* **55**, 541 (1985).  
<sup>29</sup>V. L. Pokrovsky and A. L. Talapov, *Zh. Eksp. Teor. Fiz.* **78**, 269 (1980) [*Sov. Phys. JETP* **51**, 134 (1980)]; *Theory of Incommensurate Crystals* (Harwood Academic, Chur, 1984).  
<sup>30</sup>T. Bohr, V. L. Pokrovsky, and A. L. Talapov, *Pis'ma Zh. Eksp. Teor. Fiz.* **35**, 165 (1982) [*Sov. Phys.- JETP Lett.* **35**, 203 (1982)]; T. Bohr, *Phys. Rev. B* **25**, 6981 (1982); H. J. Schulz, *ibid.* **28**, 2746 (1983).  
<sup>31</sup>When the helicity modulus is an anisotropic tensor,  $\Gamma$  in Eq. (16) stands for the geometric mean of its eigenvalues.  
<sup>32</sup>This estimate does not take into account the renormalization effects (related to the presence of bound pairs of fractional vortices), which would shift  $T_{FV}$  further down.  
<sup>33</sup>J. Villain, in *Order in Strongly Fluctuating Condensed Matter Systems*, edited by T. Riste (Plenum, New York/London, 1980), p. 221; *Surf. Sci.* **97**, 219 (1980); J. Villain and M. B. Gordon, *ibid.* **125**, 1 (1983).  
<sup>34</sup>Y. Xiao, D. A. Huse, P. M. Chaikin, M. J. Higgins, S. Bhattacharya, and D. Spencer, *Phys. Rev. B* **65**, 214503 (2002).  
<sup>35</sup>O. Sato and M. Kato, *Physica B* **329-333**, 1405 (2003).  
<sup>36</sup>P. Erdős and W. Zheng, *Phys. Rev. B* **82**, 134532 (2010).  
<sup>37</sup>S. E. Korshunov, *Phys. Rev. B* **71**, 174501 (2005).  
<sup>38</sup>S. E. Korshunov, *Phys. Rev. B* **63**, 134503 (2001).  
<sup>39</sup>T. Ishida, M. Yoshida, K. Okuda, S. Okayasu, M. Sasase, K. Hojou, A. Odawara, A. Nagata, T. Morooka, S. Nakayama, and K. Chinone, *Physica C* **357-360**, 604 (2001).  
<sup>40</sup>M. D. Stewart, Z. Long, J. M. Vallas, A. Yin, J. M. Xu, *Phys. Rev. B* **73**, 092509 (2006); H. Q. Nguyen, S. M. Hollen, M. D. Stewart Jr., J. Shainline, A. Yin, J. M. Xu, and J. M. Valles Jr., *Phys. Rev. Lett.* **103**, 157001 (2009).  
<sup>41</sup>S. Alexander, *J. Phys.* **44**, 805 (1983).  
<sup>42</sup>A. Vallat, S. E. Korshunov, and H. Beck, *Phys. Rev. B* **43**, 8482 (1991); A. Vallat and H. Beck, *ibid.* **50**, 4015 (1994).